Signal Extraction Overview

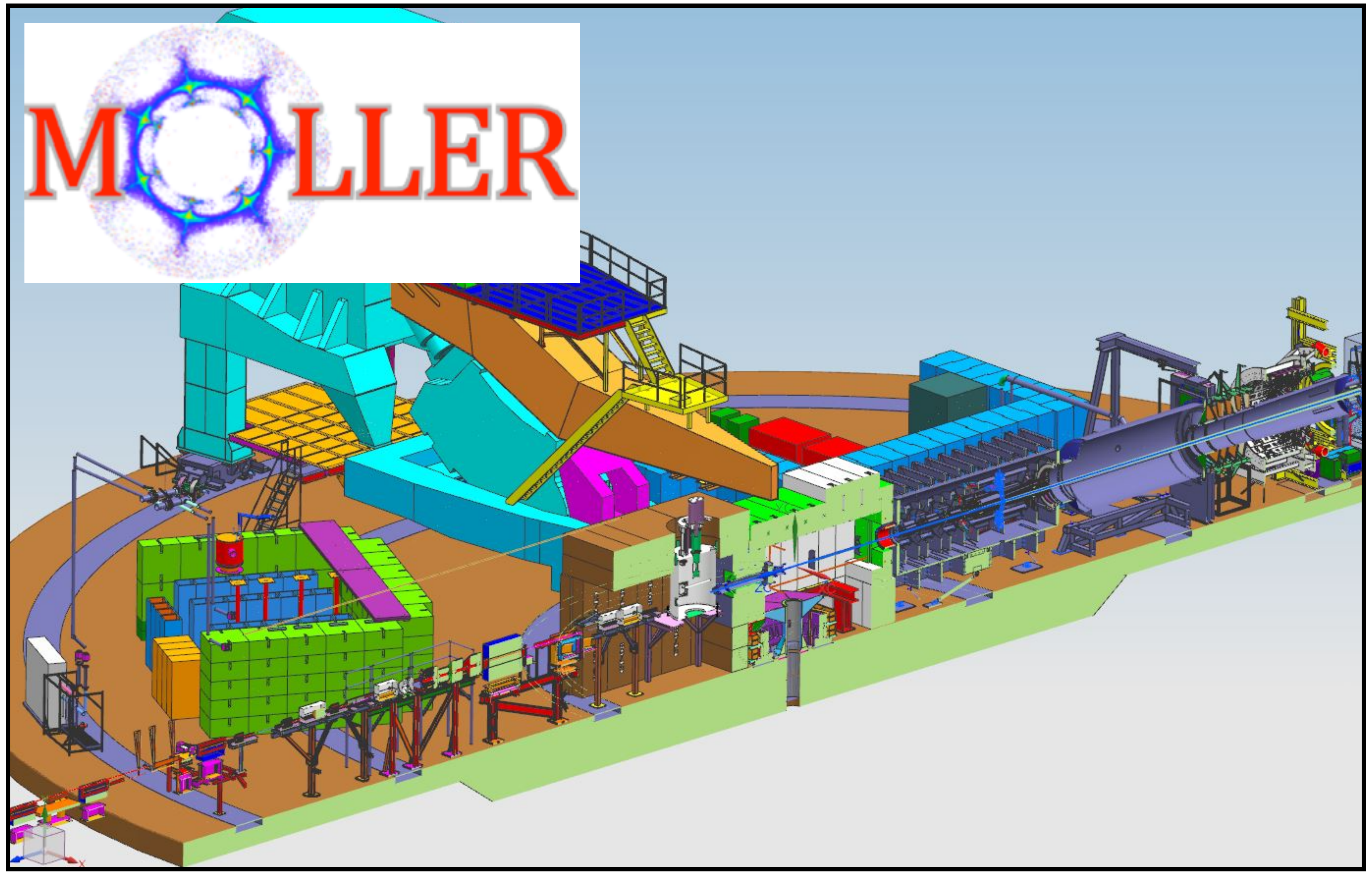

Kent Paschke
University of Virginia

July 30, 2025

Charge item 14: simulation, readiness for analysis

Extracting A_{PV} from the Measured Flux

map E-θ correlation for *ee* scattering to detector

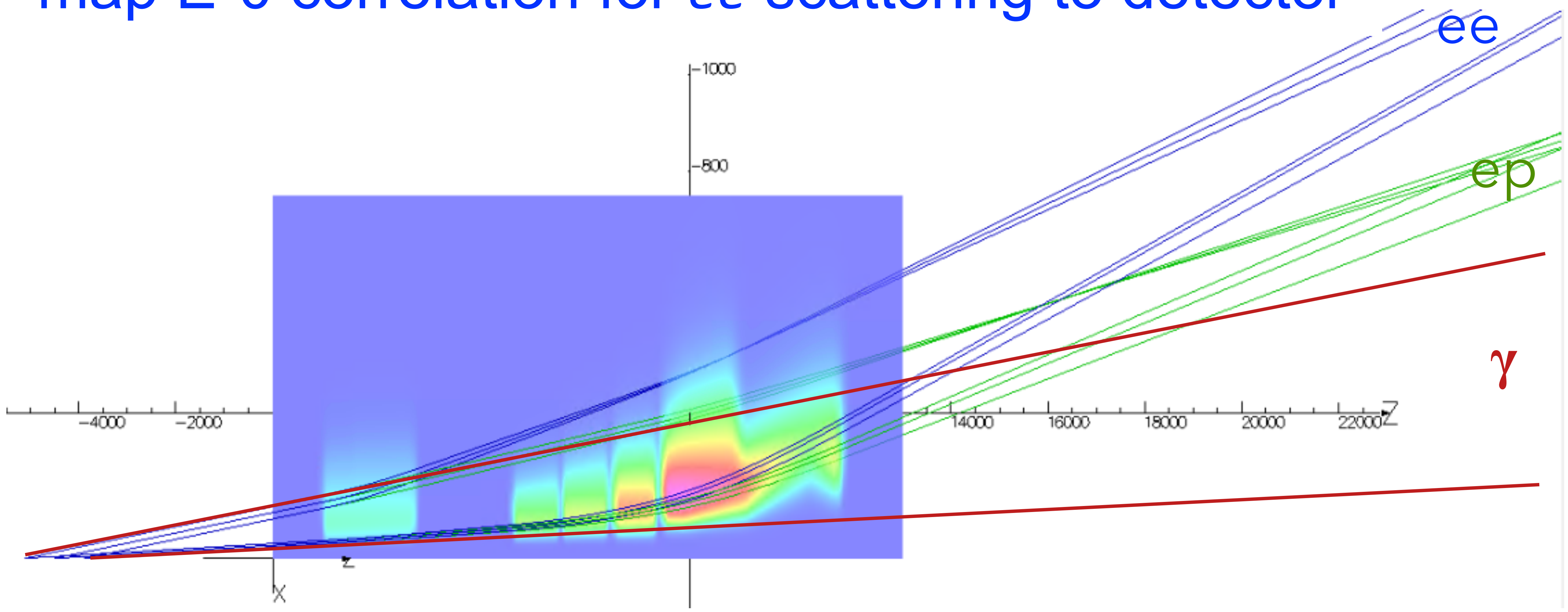

Rapid (1kHz) measurement over helicity reversals to cancel noise

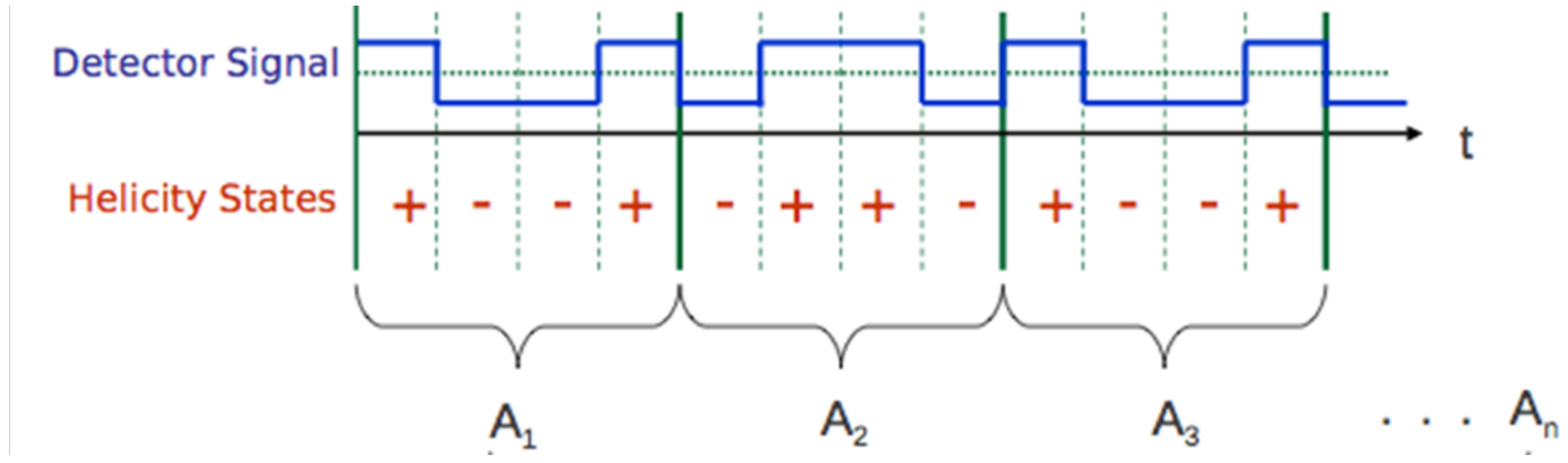

Integration of analog detector current

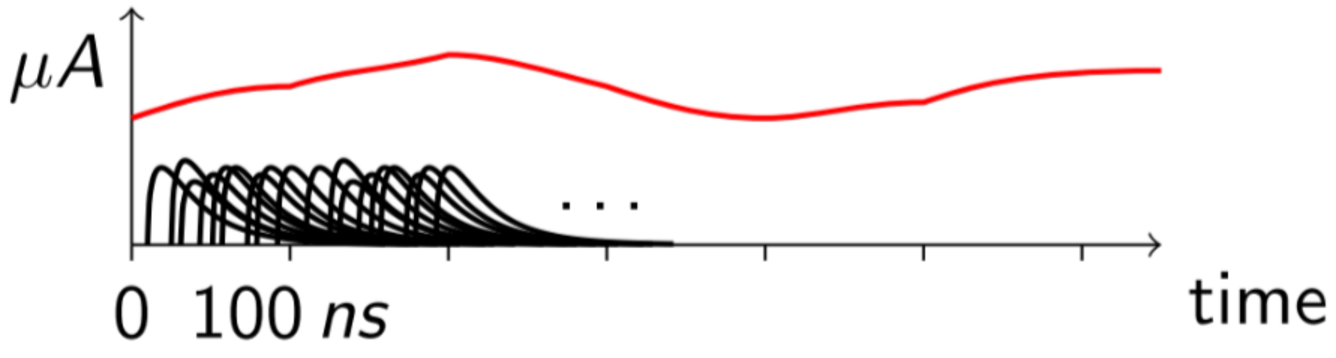

$$A_{pair} = \frac{\Delta F}{2F} + \Delta A$$

$$\left(A_{expt}\right)_i = \left(\frac{\Delta F}{2F} - \frac{\Delta I}{2I}\right)_i - \sum_j \left(\alpha_j \left(\Delta X_j\right)_i\right)$$

Corrections to measured asymmetry, variable per each measurement and essential for extracting statistical precision

$$\sigma_{pair} = \sqrt{\frac{1}{N}} \quad + \textit{noise}$$

$$\sigma_{A_{expt}} = \frac{\sigma_{pair}}{\sqrt{N_{pair}}}$$

Corrections to measured asymmetry, averaged over stable periods

$$A_{PV} = \frac{1}{P_b} \frac{A_{expt} - A_T - A_{NL} - \sum_i f_i A_i}{\sum (1 - f_i)}$$

Backgrounds (asymmetry and dilution)

Noise sources in A_{expt}

$$\left(A_{expt}\right)_i = \left(\frac{\Delta F}{2F} - \frac{\Delta I}{2I}\right)_i - \sum_j \left(\alpha_j \left(\Delta X_j\right)_i\right)$$

$$\sigma_{pair} = \sqrt{\frac{1}{N}} + noise$$

$$\sigma_{A_{expt}} = \frac{\sigma_{pair}}{\sqrt{N_{pair}}}$$

Ultimate Contributions to σ_{pair} - "Pair width"

Parameter	Random Noise (65 μA)
Statistical width (0.5 ms)	**~ 82 ppm**
Target Density Fluctuation	30 ppm
Beam Intensity Resolution	10 ppm
Beam Position Noise	7 ppm
Detector Resolution (25%)	21 ppm (3.1%)
Electronics noise	10 ppm
Measured Width (σ_{pair})	**91 ppm**

- **Statistics:** ~145 GHz. About 1/3000 of incident beam electrons create a MOLLER signal in our Ring 5 detector **(Kumar)**
- **Target density instability:** changes in luminosity due to target. Very stable target plus rapid relative measurements control this noise
- **Beam intensity:** high-resolution measurement of incident beam flux **(M. Pitt)**
- **Beam position:** high resolution measurement of beam position variations and precise calibration of the sensitivity
- **Detector resolution:** rms width of detector response adds to statistical variation in signal **(M. Gericke)**
- **Electronics noise:** will also contribute

Calibrating Corrections to Extract A_{PV}

Anticipated Uncertainty in A_{PV}

Error Source	Fractional Error (%) Run 1	Fractional Error (%) Ultimate
Statistical	**11.4**	**2.1**
Absolute Norm. of the Kinematic Factor	3	0.5
Beam (second moment)	2	0.4
Beam polarization	1	0.4
$e + p(+\gamma) \rightarrow e + X(+\gamma)$	2	0.4
Beam (position, angle, energy)	2	0.4
Beam (intensity)	1	0.3
$e + p(+\gamma) \rightarrow e + p(+\gamma)$	0.6	0.3
$\gamma^{(*)} + p \rightarrow (\pi, \mu, K) + X$	1.5	0.3
$e + Al(+\gamma) \rightarrow e + Al(+\gamma)$	0.3	0.15
Transverse polarization	2	0.2
Neutral background (soft photons, neutrons)	0.5	0.1
Linearity	0.1	0.1
Total systematic	**5.5**	**1.1**

Acceptance averaging

$$\left(A_{expt}\right)_i = \left(\frac{\Delta F}{2F} - \frac{\Delta I}{2I}\right)_i - \sum_j \left(\alpha_j \left(\Delta X_j\right)_i\right)$$

$$A_{PV} = \frac{1}{P_b} \frac{A_{expt} - A_T - A_{NL} - \sum_i f_i A_i}{\sum (1 - f_i)}$$

Target

High power, risk for source of random noise

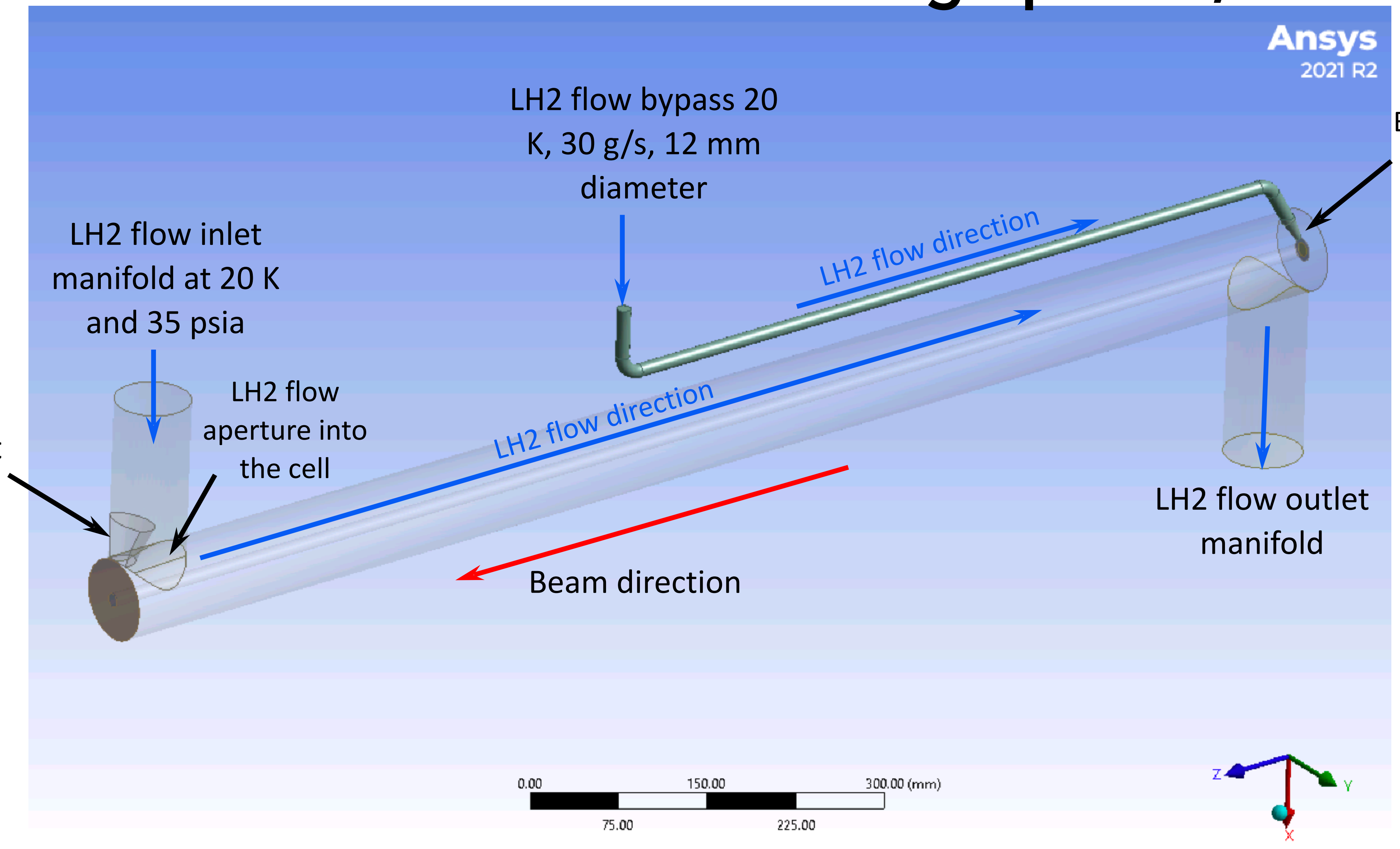

4x4 mm² raster area

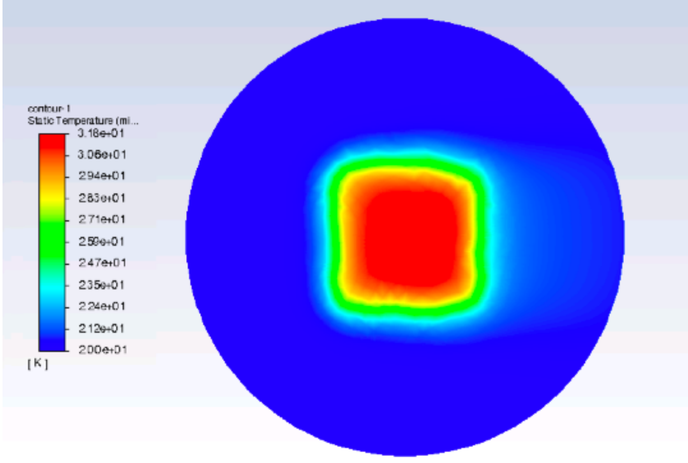

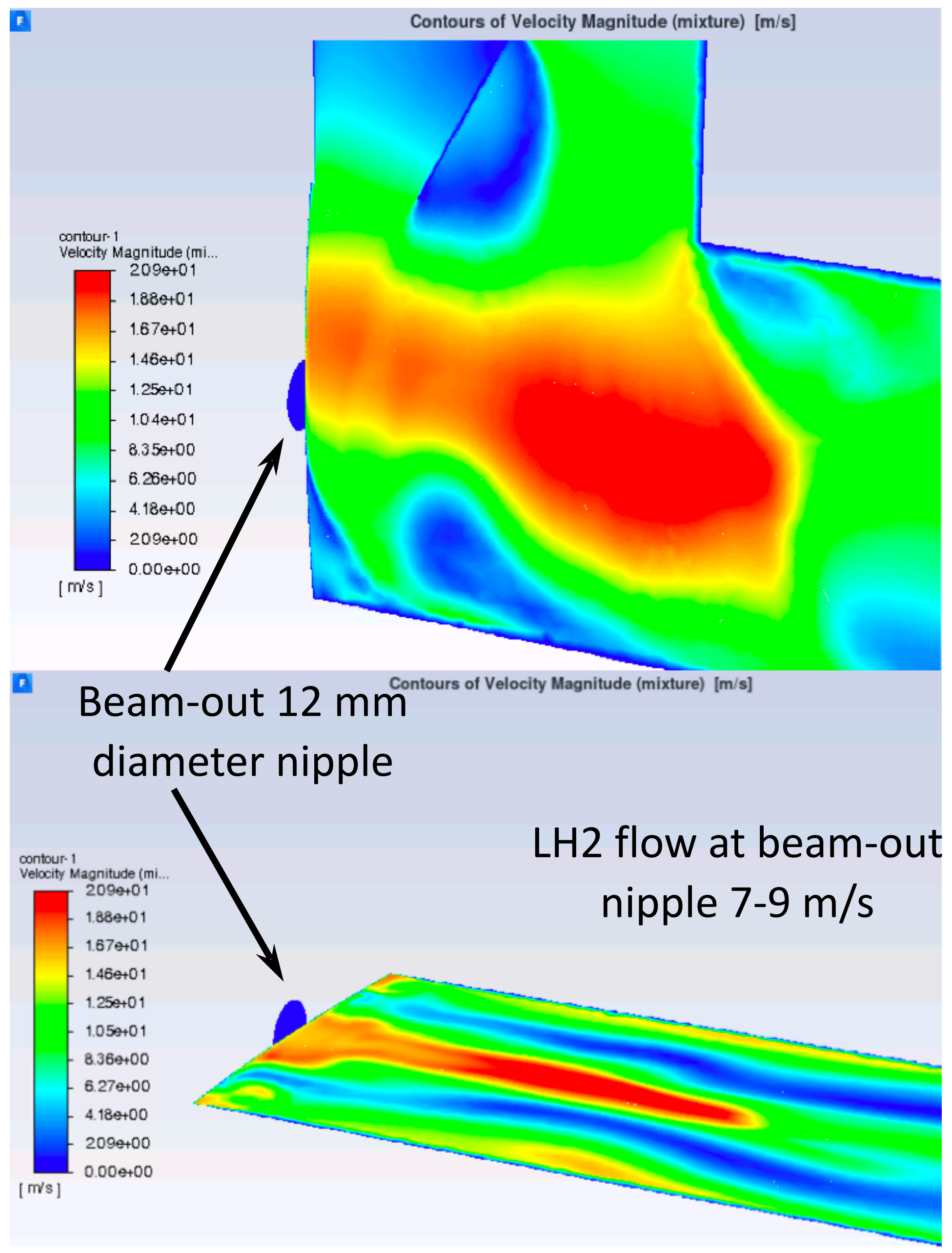

- Design informed by Qweak experience
- CFD simulations (S. Covrig Dusa)
- Jet at each window to cool dominant heat surface
- Qweak data shows noise dominated by lower frequencies, results reproduced in time-dependent CFD simulations
- CFD demonstrates design meets requirements

Fast helicity reversal (1 ms) cancels density fluctuations

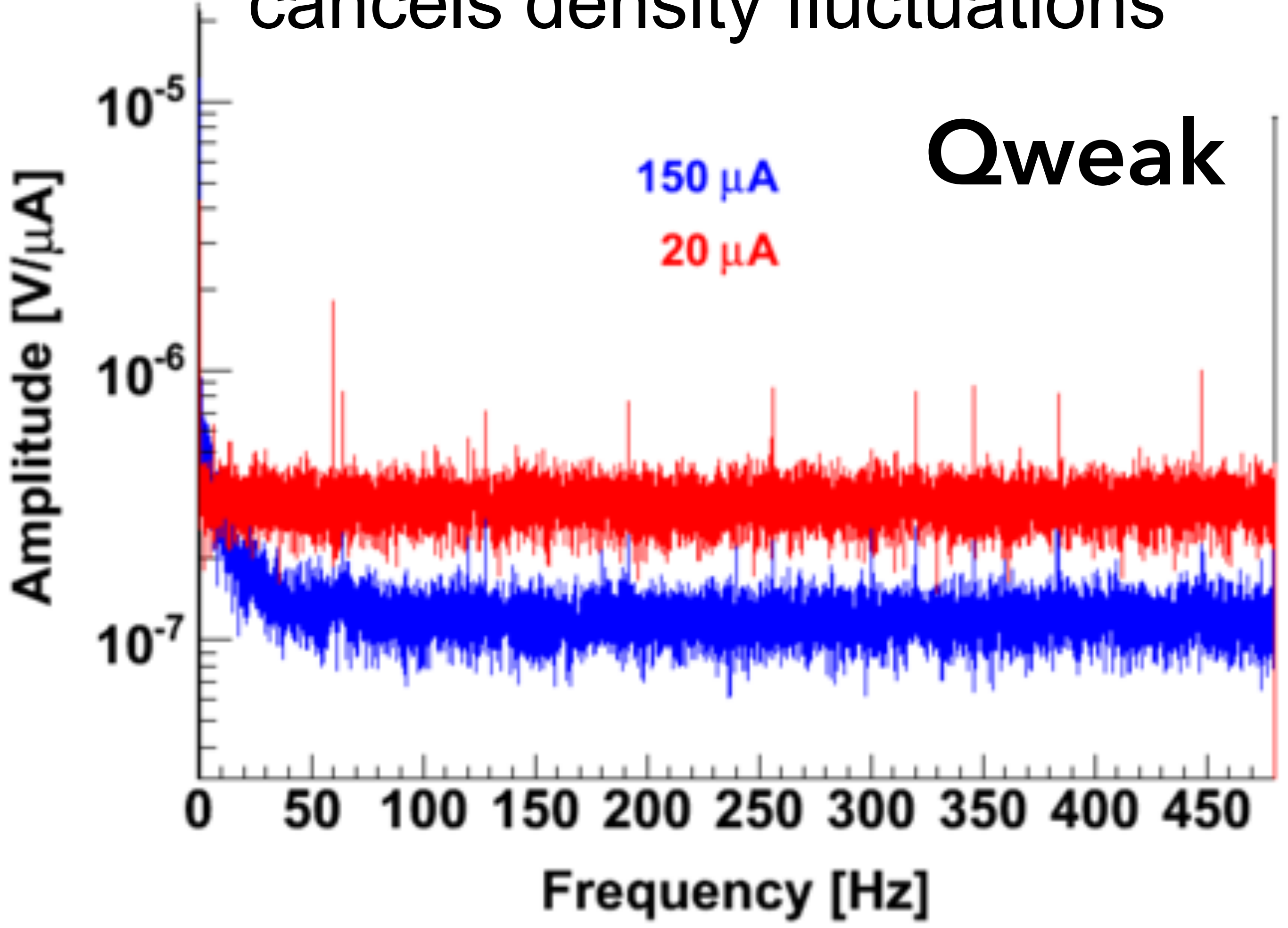

Requirements:

- $\Delta\rho/\rho$ (%) < 1%
- σ_b < 30 ppm

CFD simulation result:

- $\Delta\rho/\rho$ (%) ~ 0.85%
- σ_b < 13 ppm

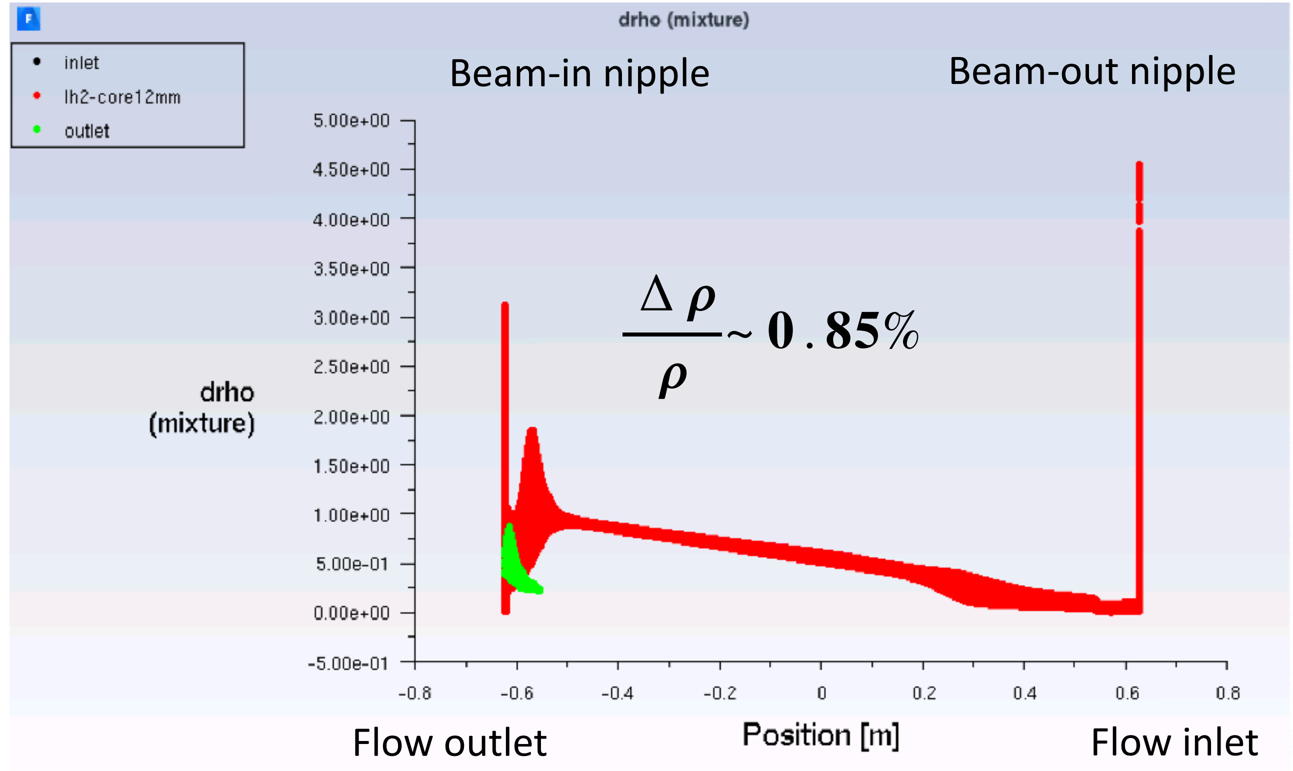

LH2 density asymmetry at 1920 Hz

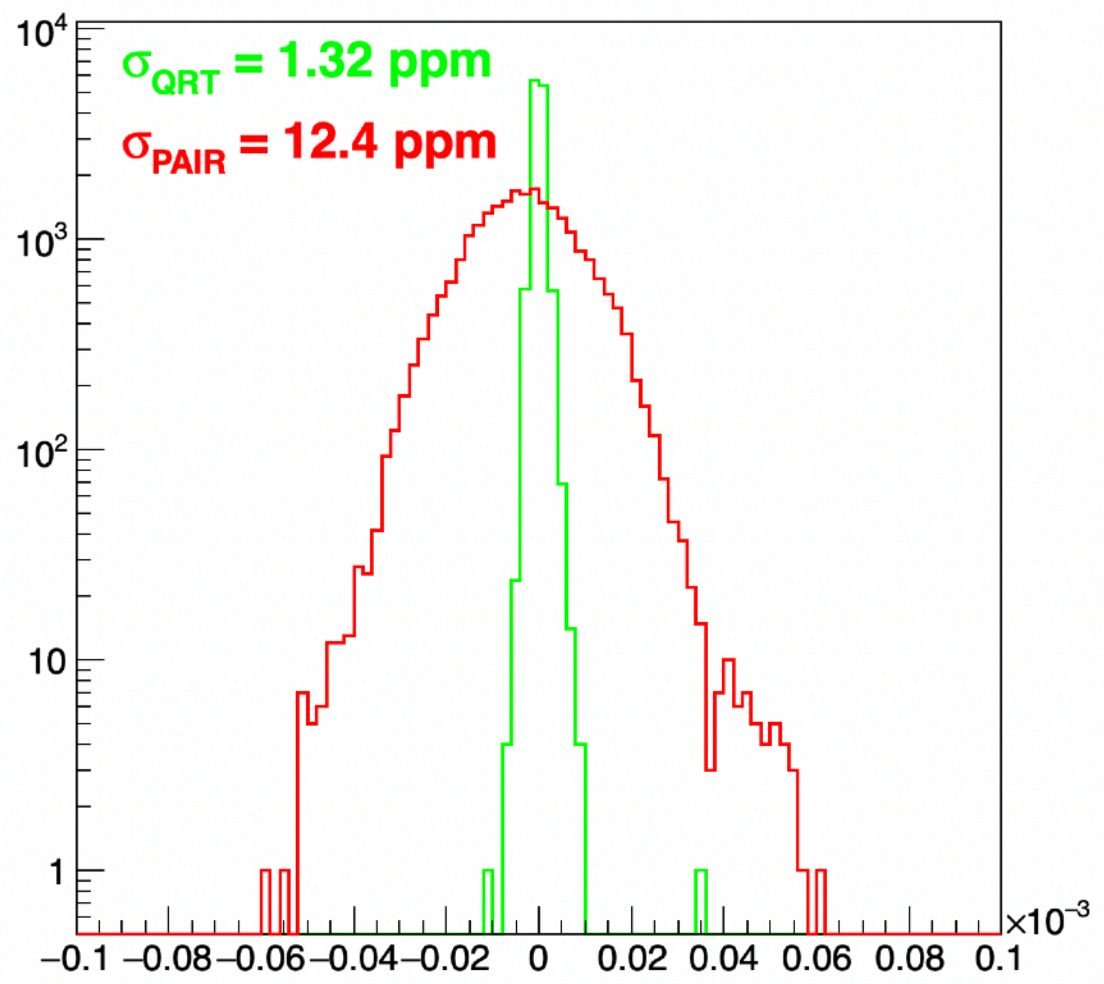

Beam Position Stability and HCBA Correction

*Must control **noise** and also possible **systematic false asymmetry** from average difference*

Correct for variations in beam intensity, position, angle, and energy fluctuations:

$$\left(A_{cxpt}\right)_i = \left(\frac{\Delta F}{2F} - \frac{\Delta I}{2I}\right)_i - \sum_j \left(\alpha_j \left(\Delta X_j\right)_i\right)$$

Random Noise:

Monitor resolution
Calibration imprecision

Parameter	Noise (65 μA)
Statistical Width	**~82 ppm**
Beam Intensity Resolution	10 ppm
Beam Position Noise	7 ppm

Systematic Correction:

Small HCBA, robust corrections

Error Source	Fractional Error (%)
Beam (position, angle, energy)	0.4
Beam (intensity)	0.3

Keep Helicity-Correlated Beam Asymmetries small

- Special techniques with the polarized source laser optics
- Beam transport configuration to avoid exacerbating differences
- “slow reversals” that flip the sign of beam asymmetries
- feedback

Beam Property	Assumed Sensitivity	Accuracy of Correction	Required 1 kHz random fluctuations	Required cumulative helicity-correlation	Systematic contribution
Intensity	1 ppb / ppb	$\sim$1%	$<$ 1000 ppm	$<$ 10 ppb	$\sim$ 0.1 ppb
Energy	-0.7 ppb / ppb	$\sim$5%	$<$ 108 ppm	$<$ 1.4 ppb	$\sim$ 0.05 ppb
Position	1.7 ppb / nm	$\sim$5%	$<$ 47 μm	$<$ 0.6 nm	$\sim$ 0.05 ppb
Angle	8.5 ppb / nrad	$\sim$5%	$<$ 4.7 μrad	$<$ 0.12 nrad	$\sim$ 0.05 ppb
Spot Size	0.012 ppb / ppm	-	-	$<$ 10 ppm	$\sim$ 0.1 ppb

Beam correction analysis

Two calibration techniques
- beam modulation for calibration
- linear regression

Combined, for precision and accuracy in the PREX-2 analysis
- Removed >90% noise
- 4% precision on total correction

Beam Position Corrections

Multivariate Regression:

$$\chi^2 = \sum \left(A_{raw} - \sum_i \beta_i \Delta M_i \right)^2, \quad \frac{\partial \chi^2}{\partial \beta_i} = 0$$

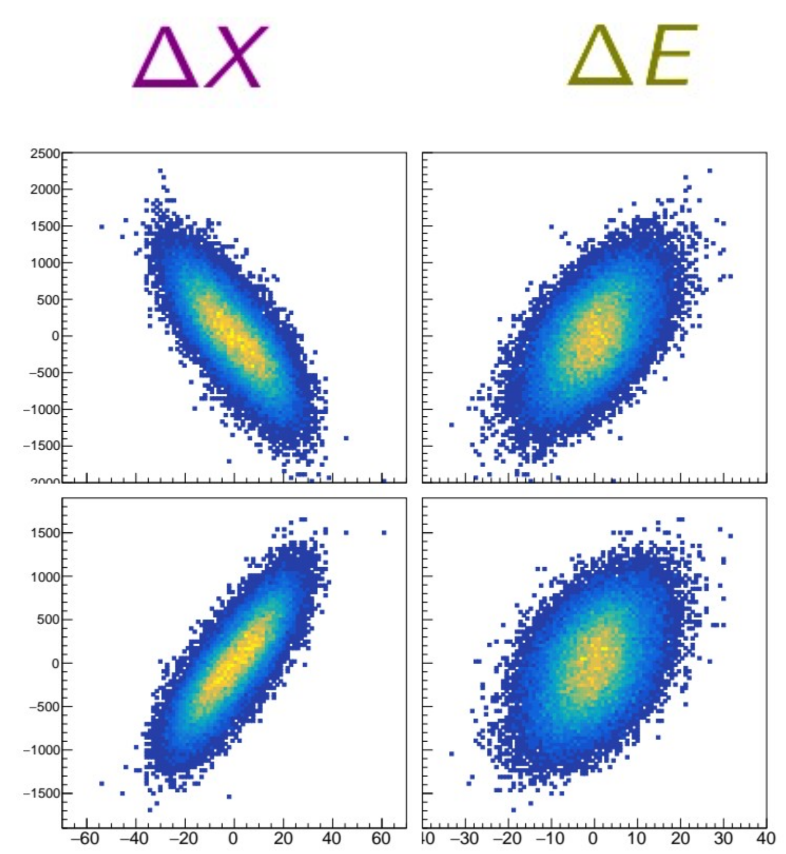

Rapid calculation, high precision, but potential bias through correlated instrumental noise

Driven Modulation:

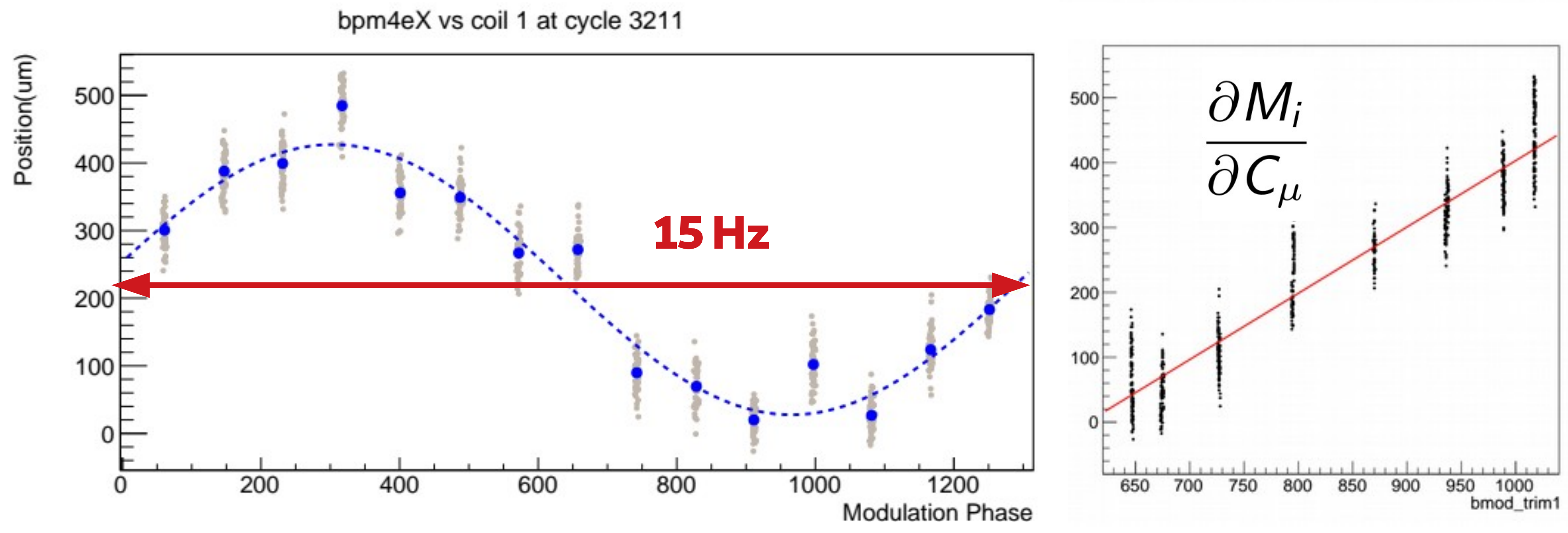

Driven modulation of beam, long update period and reduced precision, but insensitive to electronic noise

Regression constrained by beam modulation:

- Rapid calculation, high precision, but beam modulation removes bias
- Developed and successfully used during challenging PREX-2 measurement
- Multiple techniques used to calibrate and cross-check correction factors

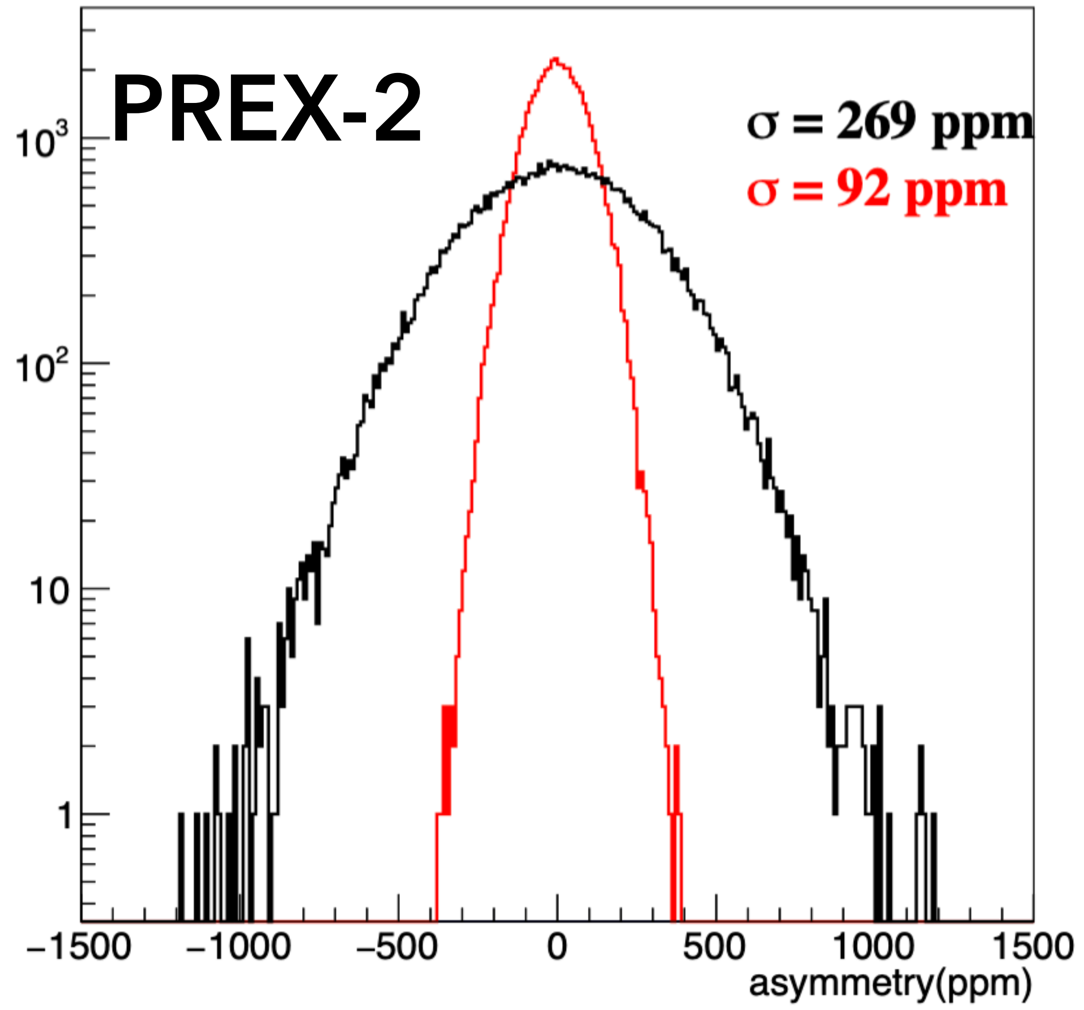

Control of HCBA

(C. Palatchi)

Source configuration
- Large body of work with polarized source and injector
- Performance, characterization and alignment of polarized source components and injector beam optics

Slow Reversals
- Includes laser optics reversals (e.g. IHWP)
- Net factor ~10 suppression of beam asymmetries

Injector Spin Manipulation
- Solenoids + 2 Wien rotations
- ~80 reversals during run phase 2&3 (weekly)

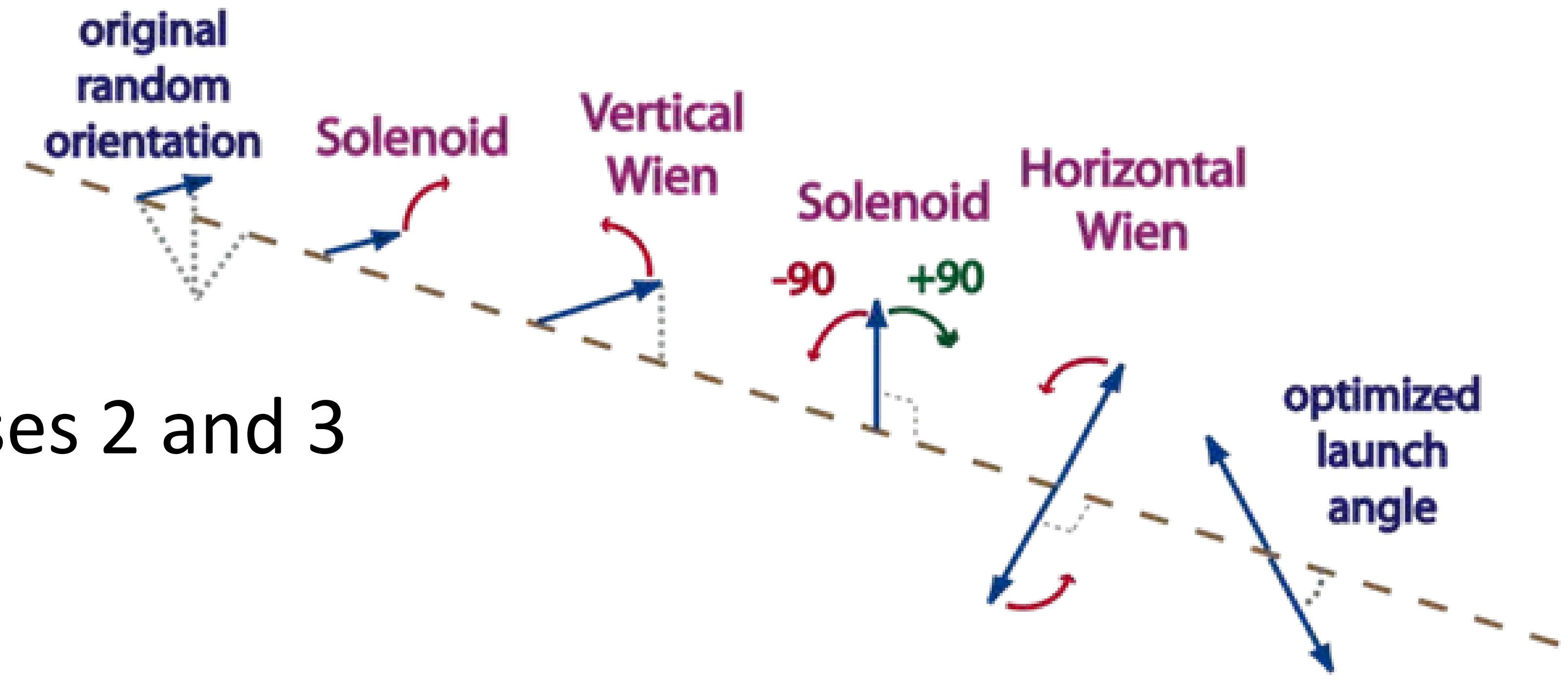

g-2 rotation
- Beam energy (ΔE~100 MeV)
- ~few reversals during run phases 2 and 3

Adiabatic Damping
- Good beam match keeps variation small

Path to meeting MOLLER goals

	Source	Adiabatic Damping	Slow Reversals	Feedback
Intensity	**<10 ppm (injector)**	-	**~10x**	**100x**
Position/ angle	**~20 nm (injector)**	**~100x (150x max)**	**~10x (IHWP, g-2, ISM)**	**~10x, control jitter**
	(Past: 30-200 nm)	Past: 5-30x (95x max)	Past: ~10x IHWP, ISM	Past: ~10x, not often used
Spot Size	**(source) $\Delta\sigma/\sigma$ <10^{-5}** Past: $\Delta\sigma/\sigma$ <10^{-4}	~10x synch light	**~10x (IHWP, g-2, ISM)**	—

Aggregation and slow reversals

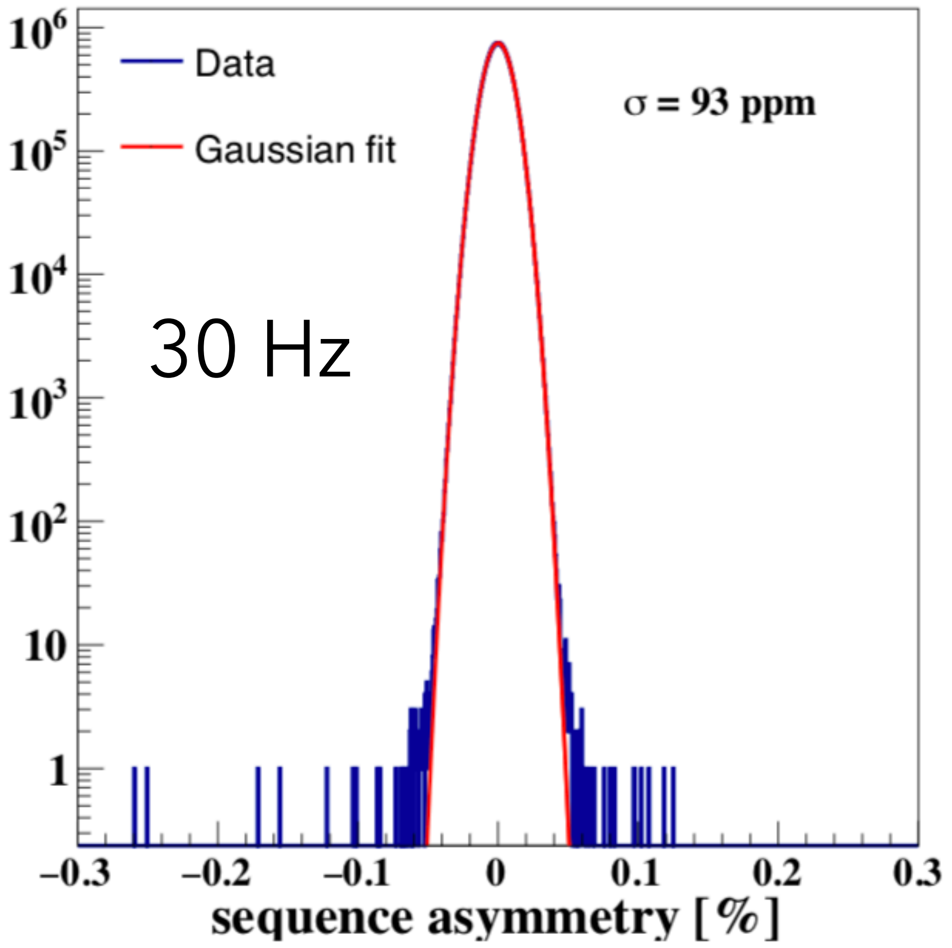

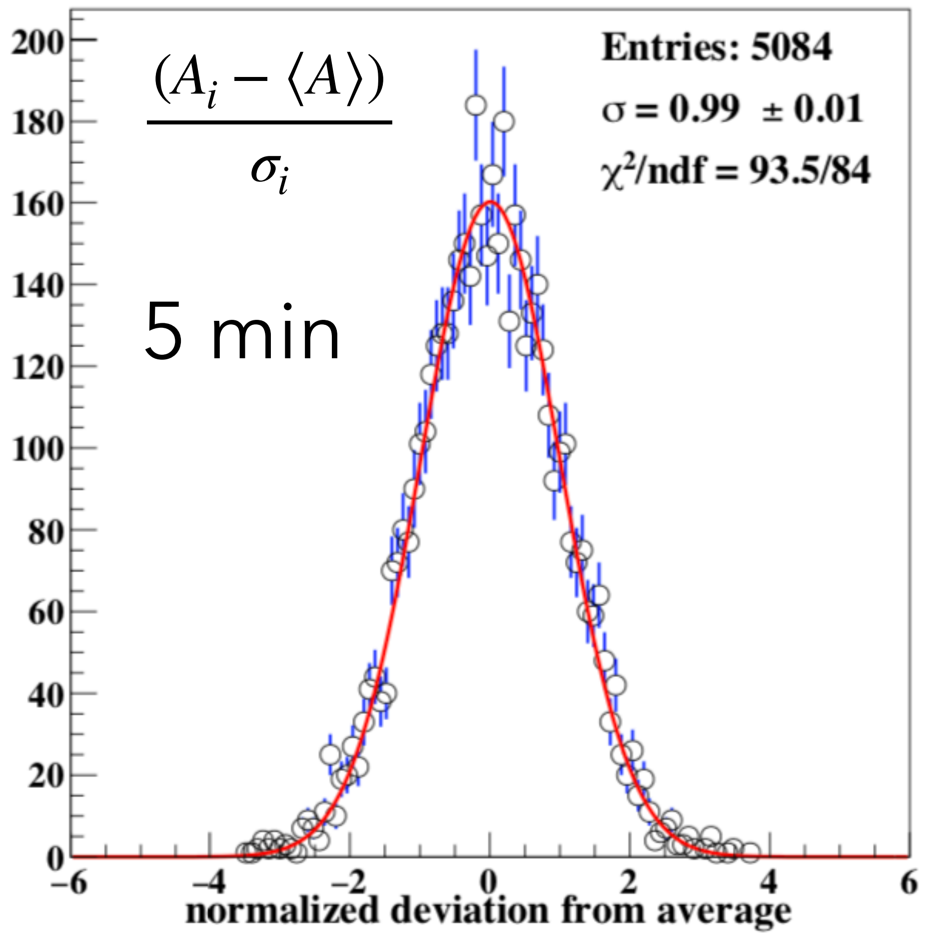

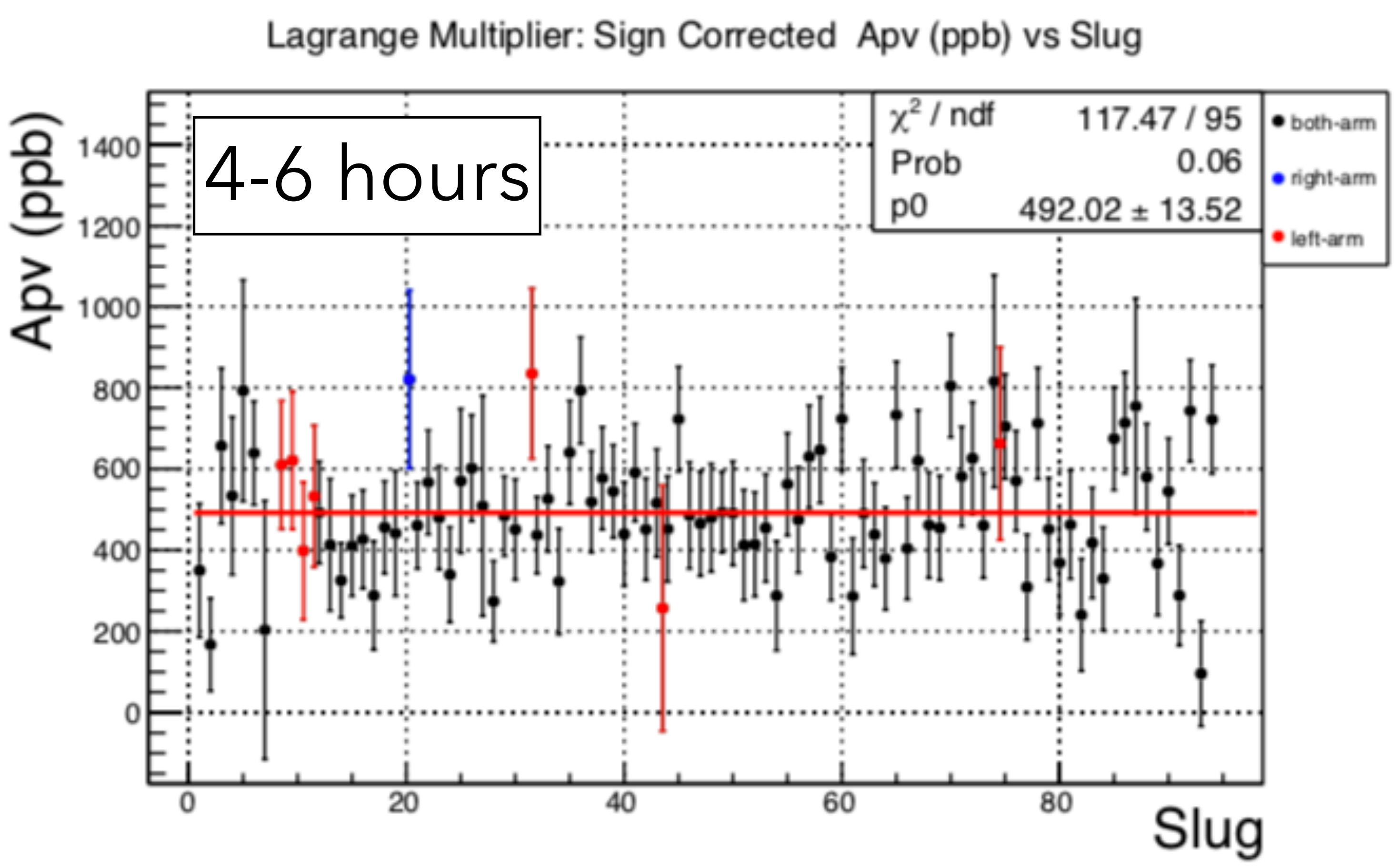

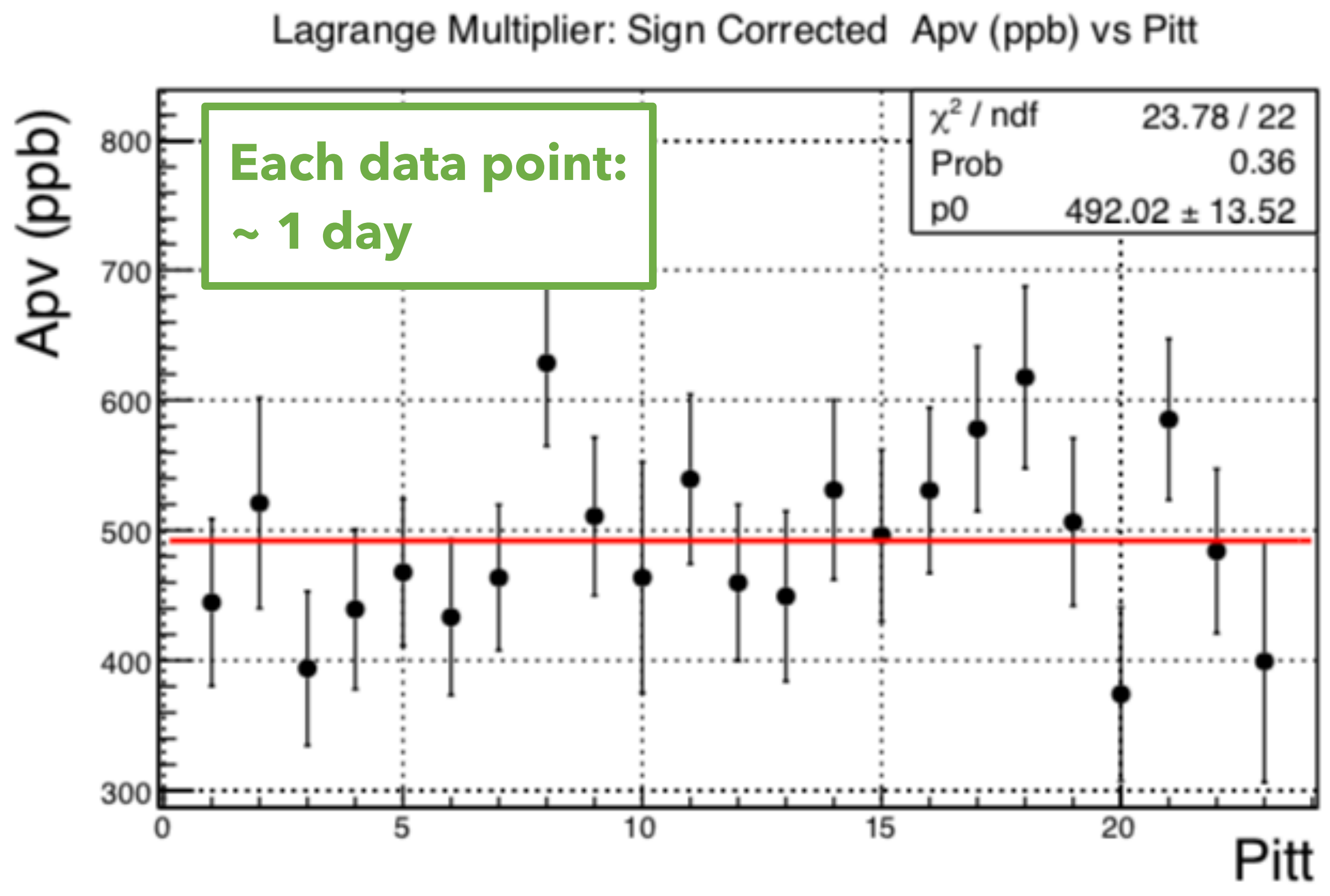

PREX data aggregated →

(noise) (systematics)

		~20PAC days	~40PAC days	344PAC days	14PAC days
		PREX-2 (achieved)	CREX (achieved)	MOLLER (required)	Cumulative Helicity Correlation (Run1)
Aq	Intensity asymmetry	25 ppb	−88 ppb	10 ppb	< 40 ppb
ΔE/E	Energy asymmetry	0.8 ± 1 ppb	0.1 ± 1.0ppb	< 1.4 ppb	< 6 ppb
Dx	position differences	2.2 ± 4 nm	-5.2 ± 3.6nm	0.6 nm	$< 4 \times 10^{-9}$ m
Δθ	angle differences	$< 0.6 \pm 0.6$ nrad	-0.26 ± 0.16nrad	0.12 nrad	$< 0.5 \times 10^{-9}$ radian
A_σ	size asymmetry (quoted)	$< 3 \times 10^{-5}$	$< 3 \times 10^{-5}$	$< 10^{-5}$	$< 10^{-5}$

Did we achieve HCBA goals? We can't tell without aggregating to achieve precision

- Aggregated results must be tested for statistical consistency, unexpected correlations, etc.
- Systematic tests are more precise with longer integrate times, but then reduce the number if independent periods to compare…
- Studies with aggregated data are an important part of the MOLLER data evaluation (**S. Park**)

Transverse Polarization Control

$$A_{PV} = \frac{1}{P_b} \frac{A_{expt} - A_T - A_{NL} - \sum_i f_i A_i}{\sum (1 - f_i)}$$

Transverse beam polarization has a left/right analyzing power

- Well known (both measured and calculated) for *ee* scattering, large in magnitude relative to A_{PV}
- Cancels over azimuthal acceptance, but must be controlled to avoid contributions from imperfect cancellation
- Zero at 90° center of mass, so detector segmentation will have a clear signature for non-zero transverse polarization

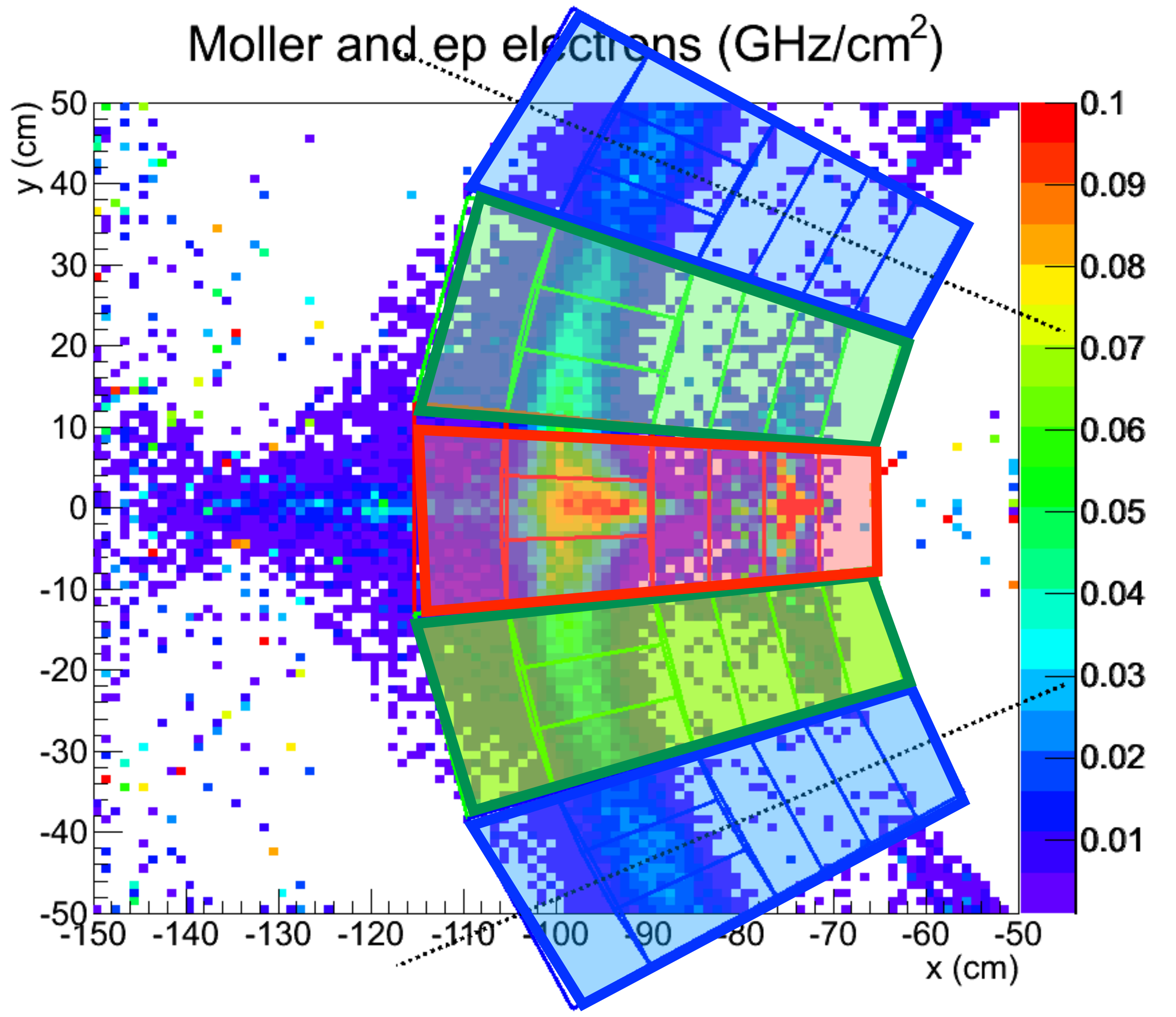

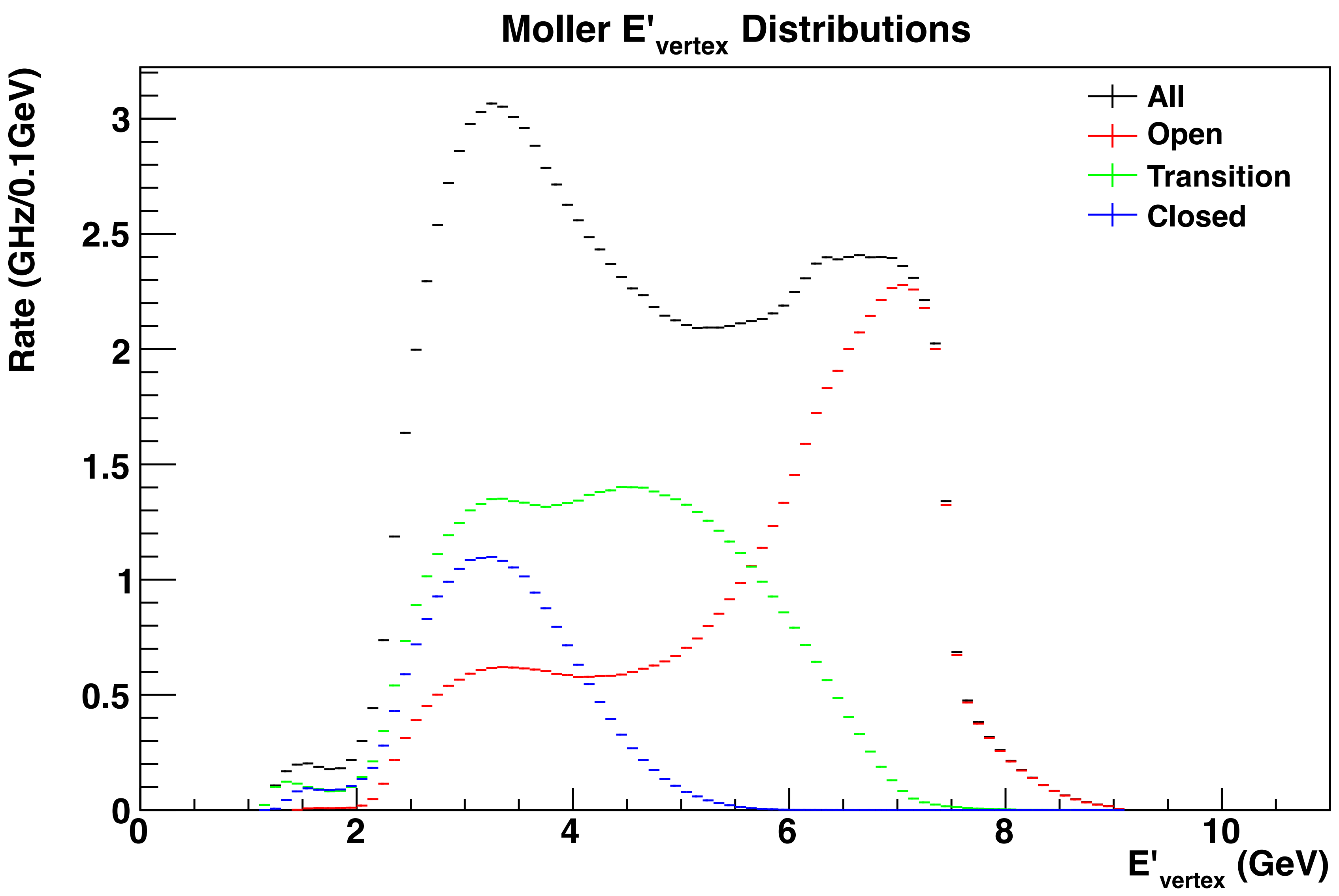

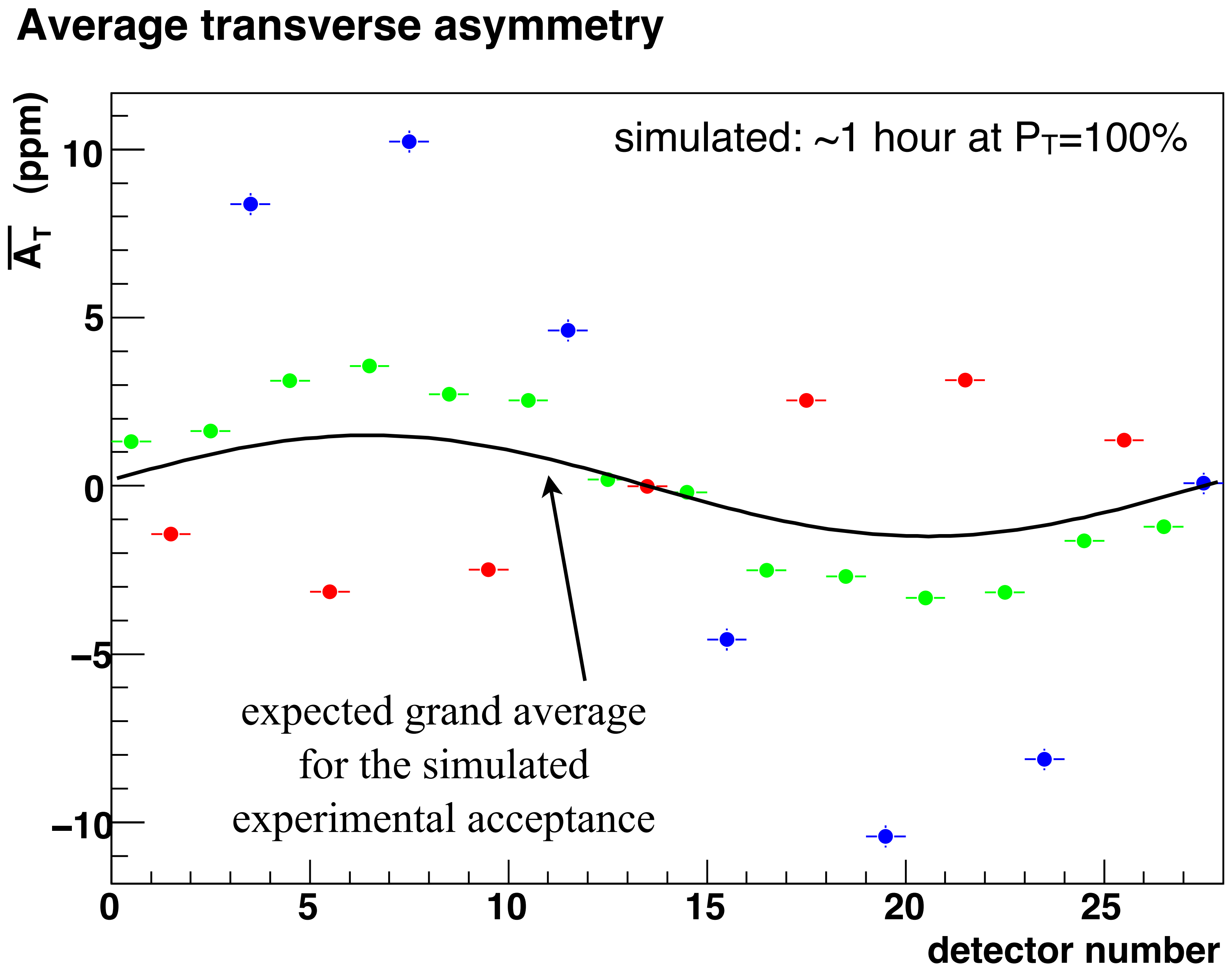

- Initial beam setup ~ 1-2 degrees
- Unique signature of transverse beam polarization
- 50 ppb error on A_T*P_b in 4 hours: 1 degree precision
- Over entire run: feedback with precession angle will hold transverse polarization small (<<1 degree)

Run Phase 1:

- A_T measurement
- Feedback technique tested

Run Phases 2 and 3:

- Routine feedback

Shielding and Collimation

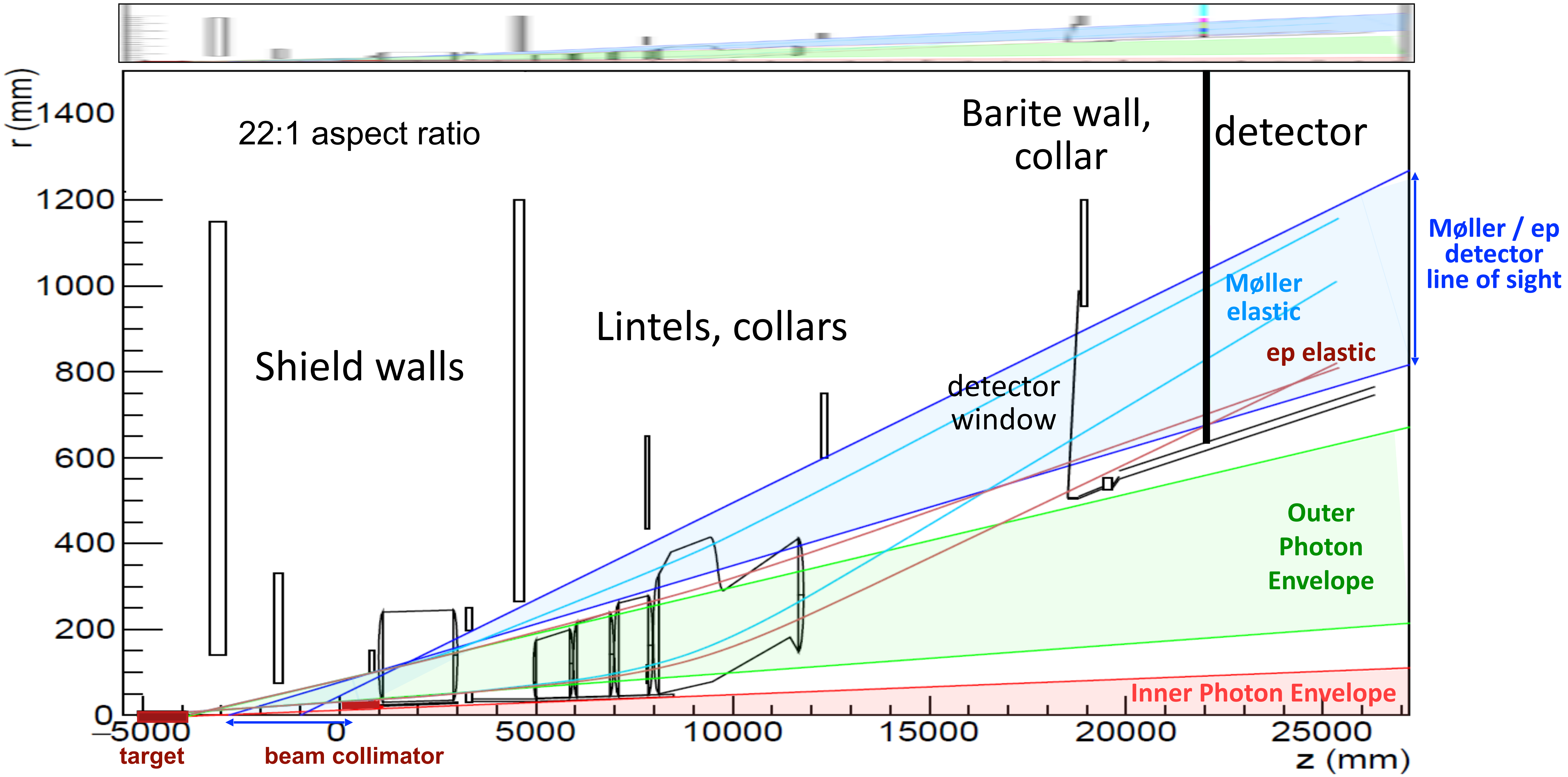

Irreducible background: radiated and/or inelastic ep or aluminum scattering, pions

Reducible background: rescattering from photons (2-bounce design), beam line, or radiative tail *e*± from target

Hygiene on reducible background sources is a major focus

Relatively small "source" terms for re-scattering could create difficult-to-model backgrounds

Simulation

remoll - GEANT 4 simulation package, gdml geometry markup 2013

- Developed in 2013
- Generators:
  - Moller, ep elastic, inelastic, Al elastic and inelastic
  - Electron “beam” generator
  - Secondary simulation (generating from input file of G4 hits)
- Detailed geometry, kept up to date with final design

Used in a wide range of studies: Design, acceptance, rates, reducible and irreducible backgrounds, ferrous materials, beam trajectory sensitivity, radiation dose rates, power deposition, spectrometer optics, light collection. Will be used to generate mock data for counting analysis design

fluka - Used for activation studies

Examination of Reducible Backgrounds with remoll

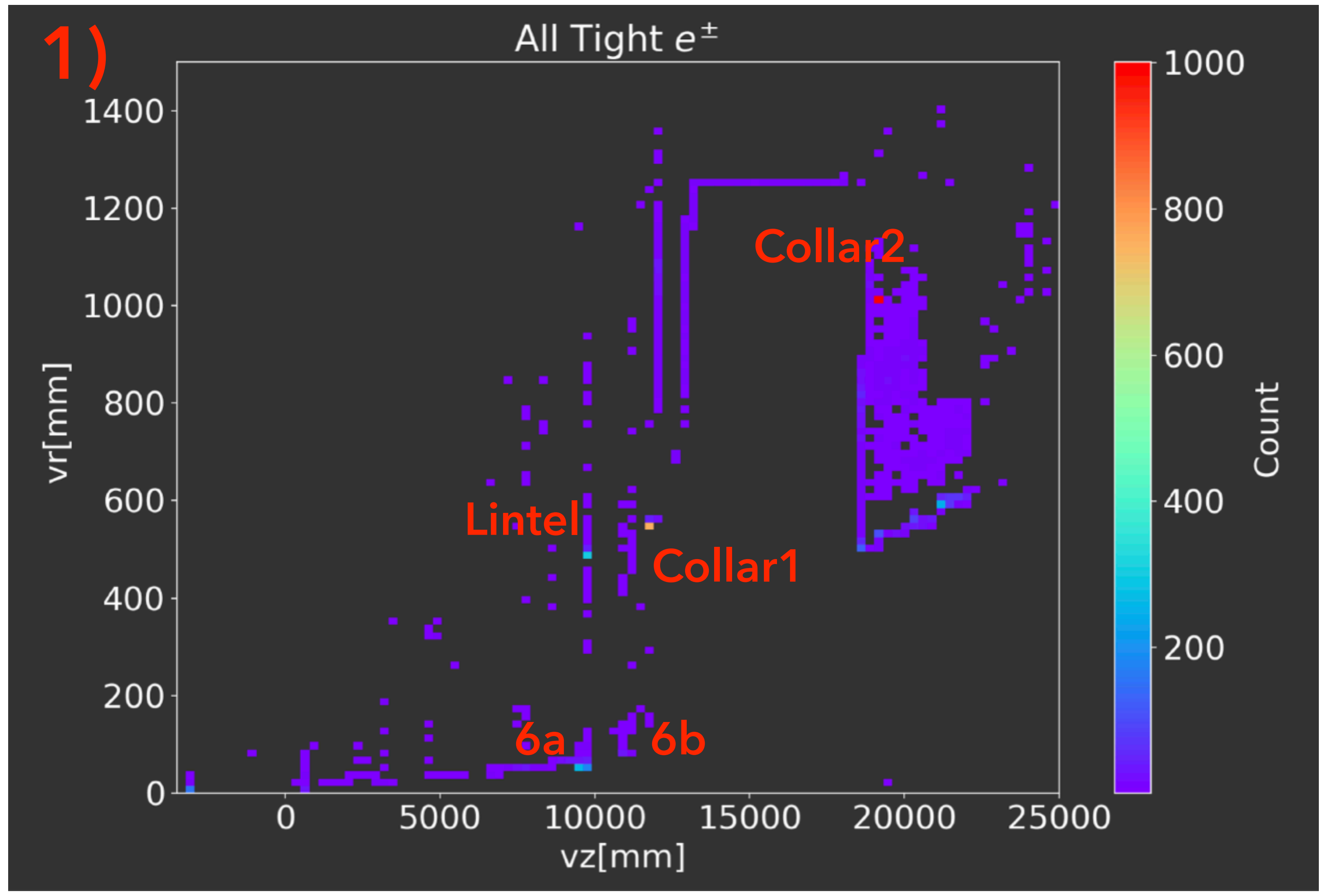

1) 2-D background heatmap
2) all background sources, showing leading sources
3) track angle vs radius at Collar 1
4) 6a vs 6b coverage

- Counting mode studies can diagnose leading sources (collars 1 and 2, collimator 6a)
- Beamline rescattering can be studied with blocked collimator
- Auxiliary detectors (LAMS, SAMS, DBMs), Ring 1 will help monitor for unexpected background sources.

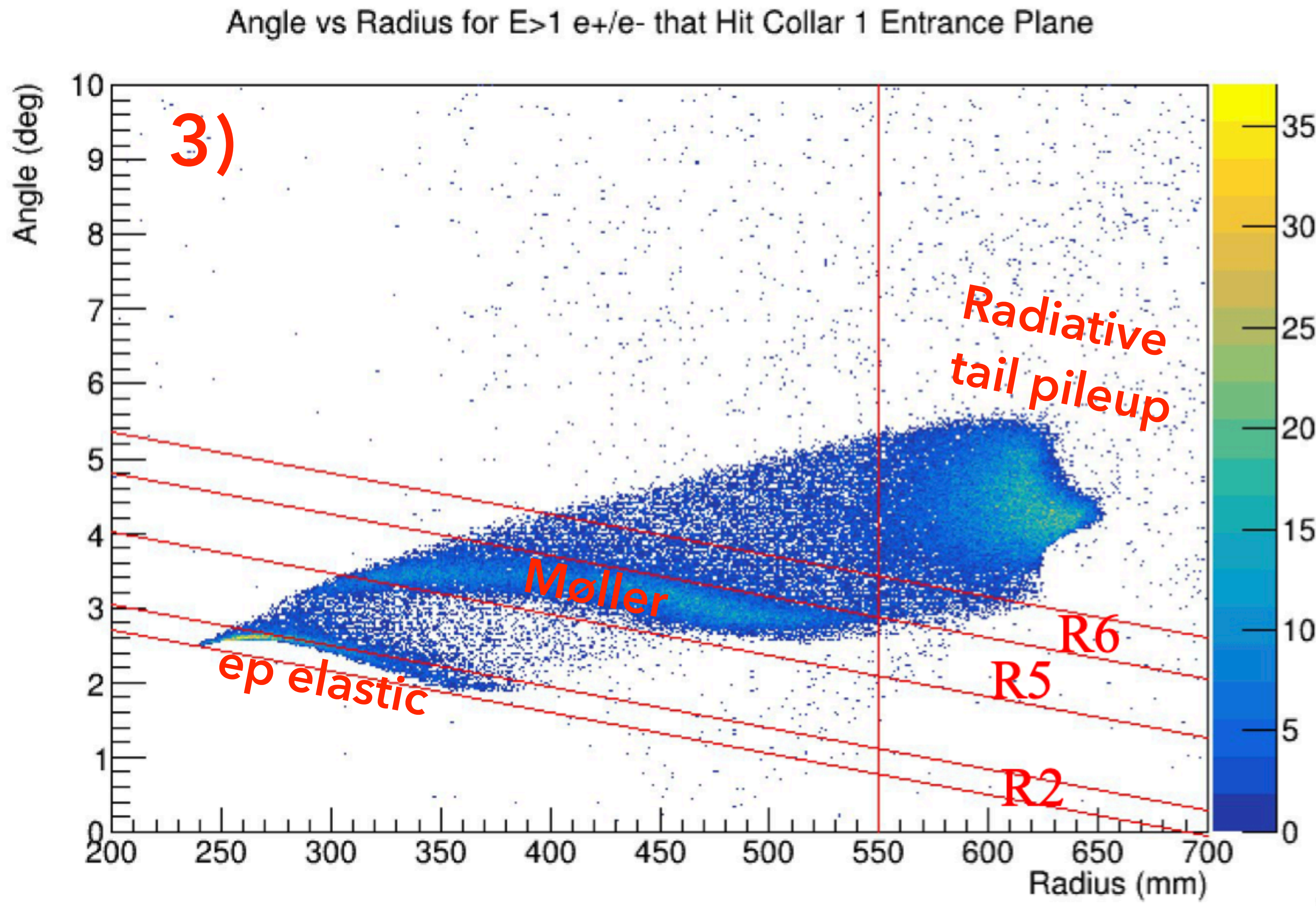

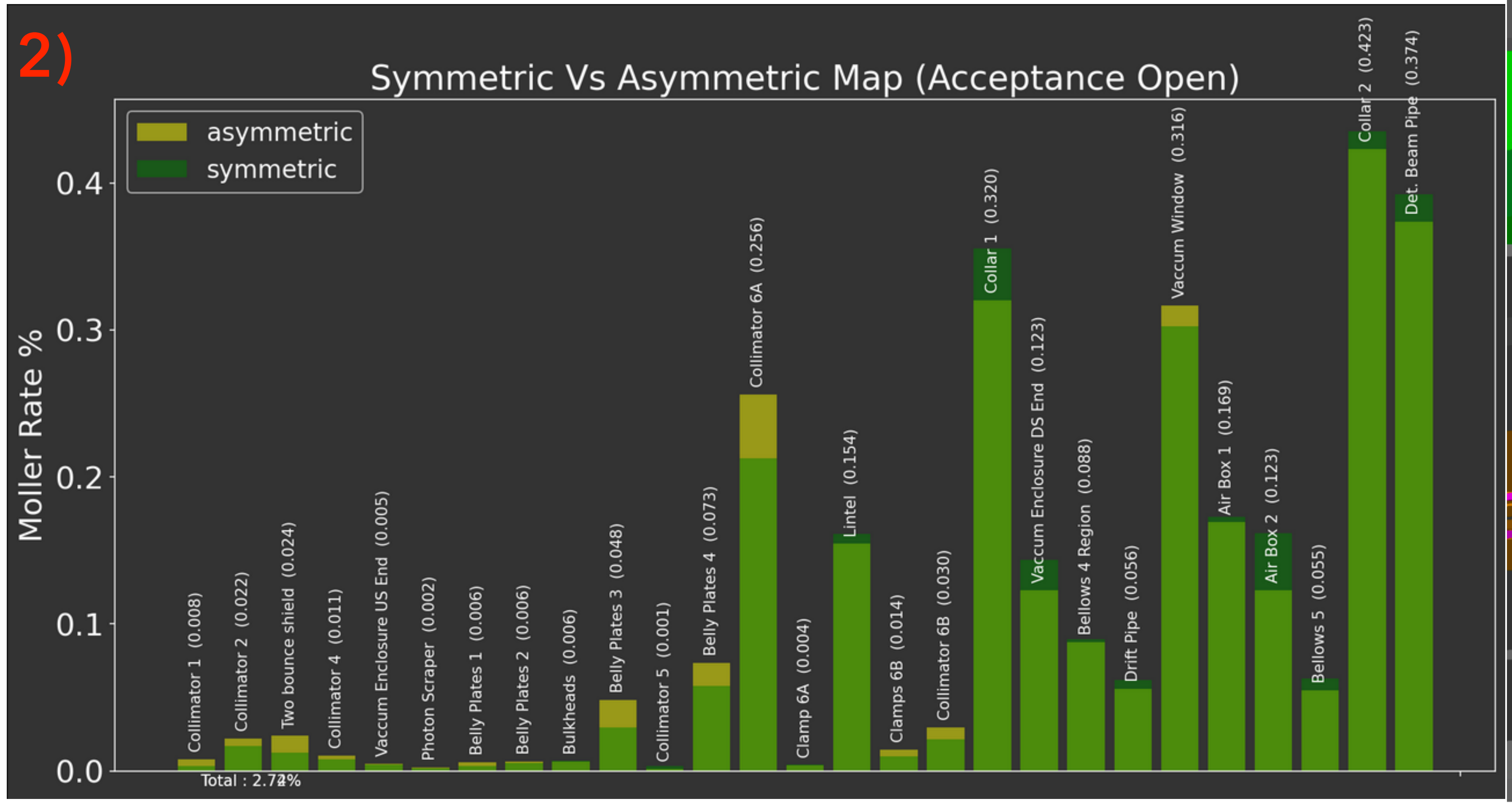

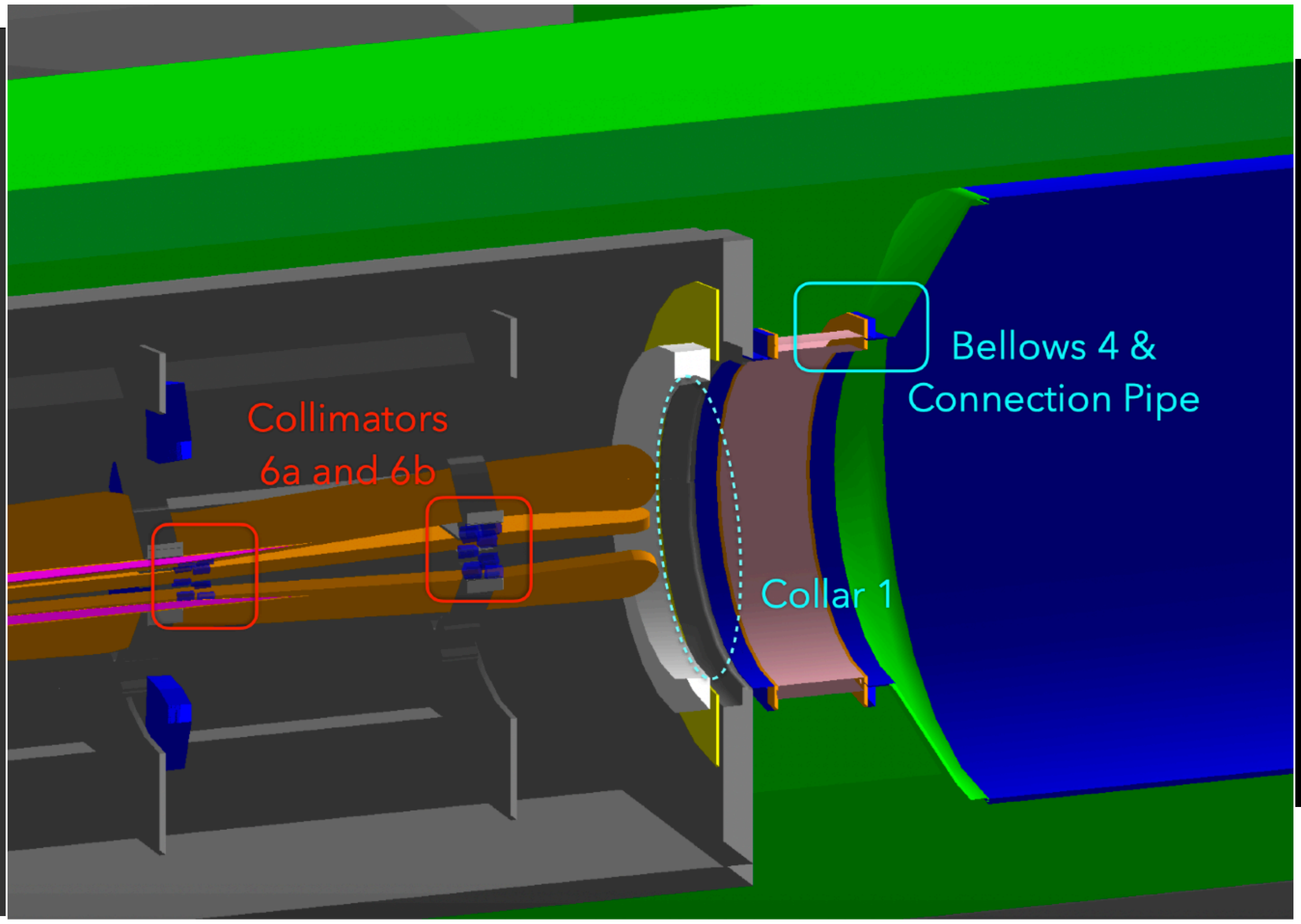

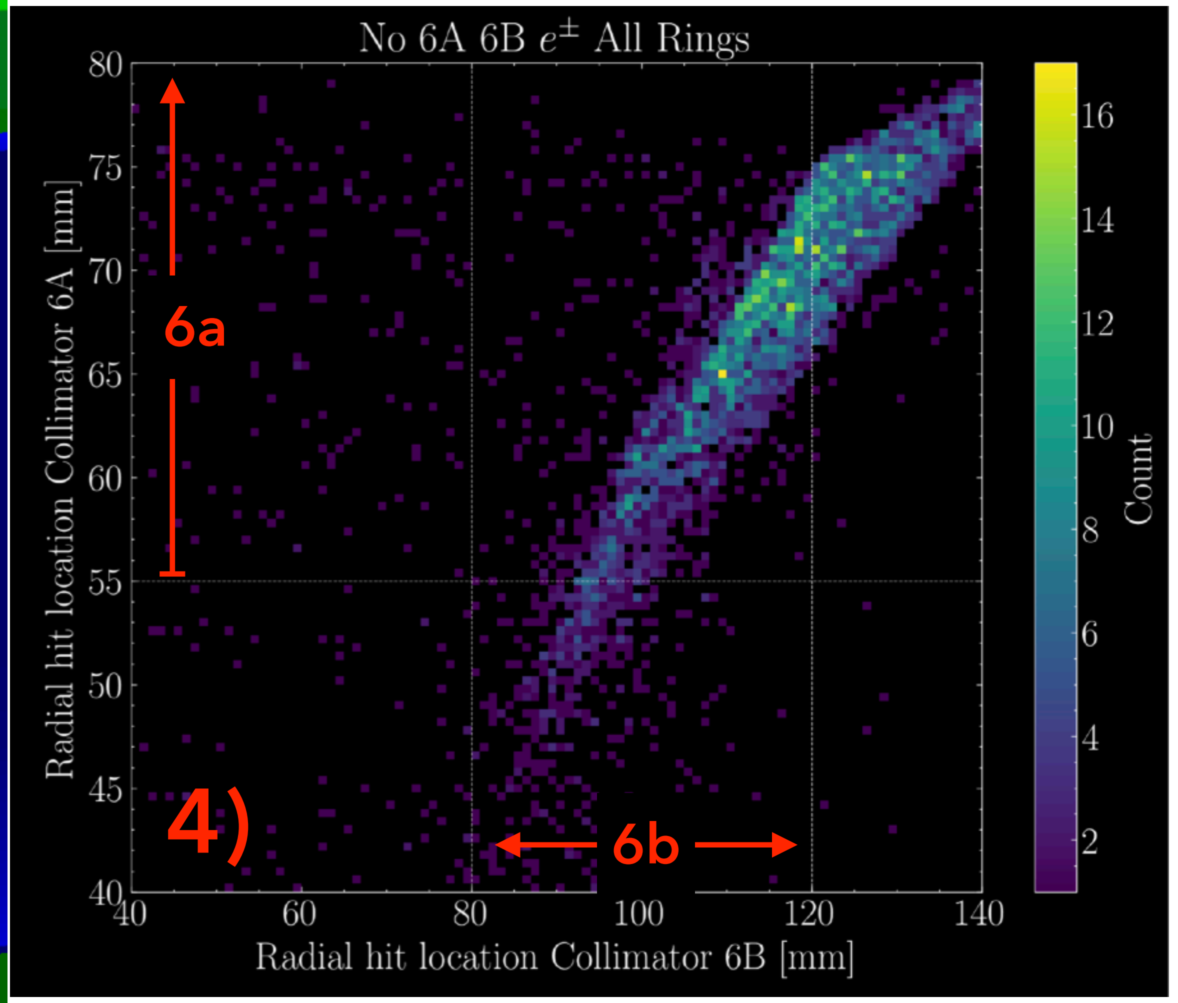

Ferrous Materials

Double-spin ee or γe scattering from ferrous material can have large asymmetry.

Goal: $A_f < 10^{-11}$

Estimate false asymmetry A_f as

$$A_f = f_r P_e P_s A_n$$

f_r rate fraction of process
P_e incident electron polarization
P_s material electron polarization
A_n analyzing power

Conservative estimates: $A_n \sim 10^{-3}$, $P_e \sim 0.3 - 1$

P_s in ~1G ambient field:

- mild steel: ~10^{-2}
- Stainless steel: ~10^{-5}-10^{-7}
- Inconel 625: ~10^{-8}
- Aluminum (paramagnetic): $< 10^{-9}$

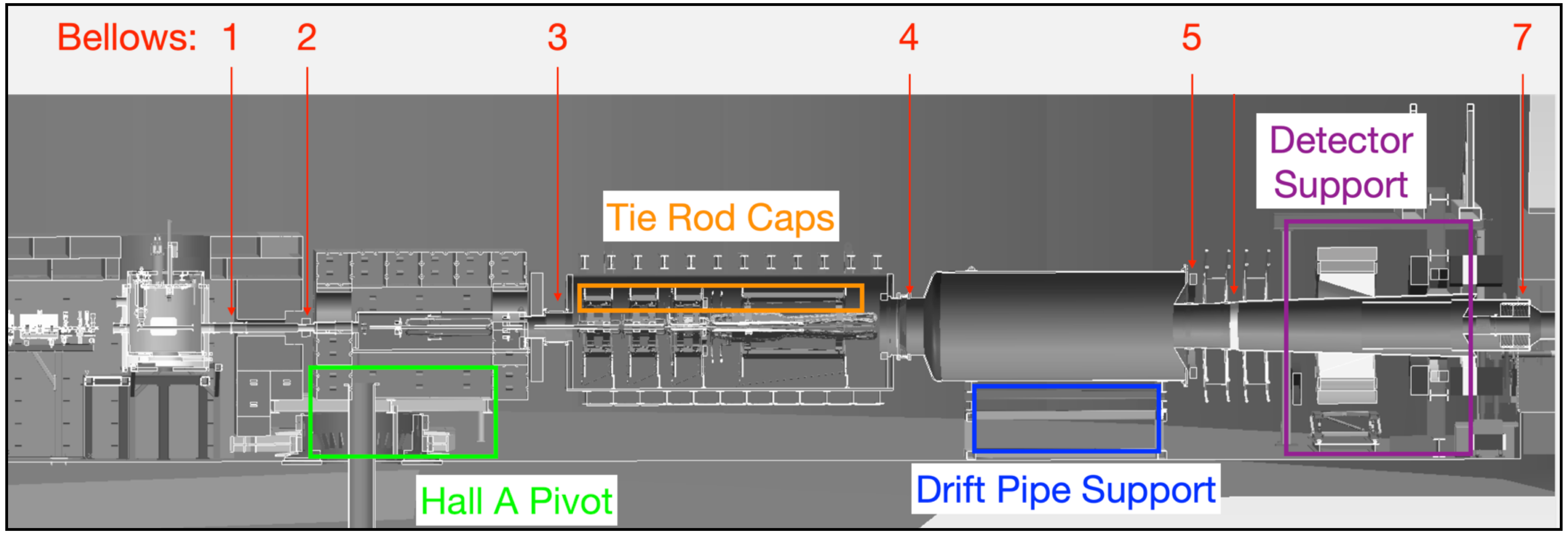

$\longrightarrow$ **f_r bound of 10^{-2} -10^{-9} corresponds to 10^{-6}-10^{-13} absolute rate**

Simulations in G4, using *ad hoc* "biasing" for rare event estimation

Examples: Bellows, pivot and HRS structure, coil support hardware in high fields, rebar, support frames, motors and power supplies, vacuum and water connections

Resulting in: new shielding, materials specifications, and other design modifications to control technical risk

Irreducible Backgrounds and Deconvolution

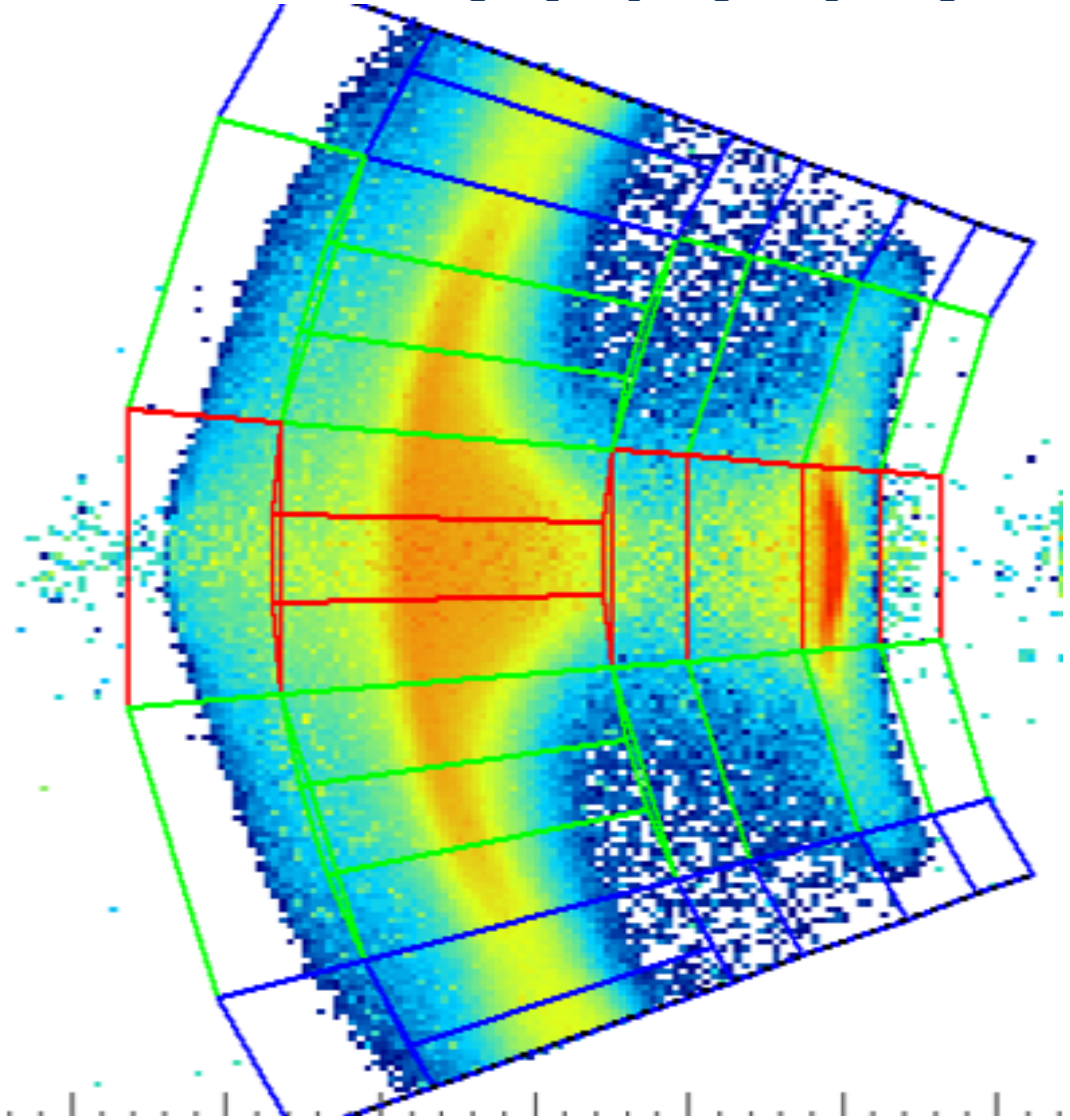

Radial distributions at the front of the detector array

- e-e scattering
- elastic e-p scattering
- inelastic e-p scattering
- elastic e-Al scattering
- inelastic e-Al scattering
- Al quasi-elastic scattering

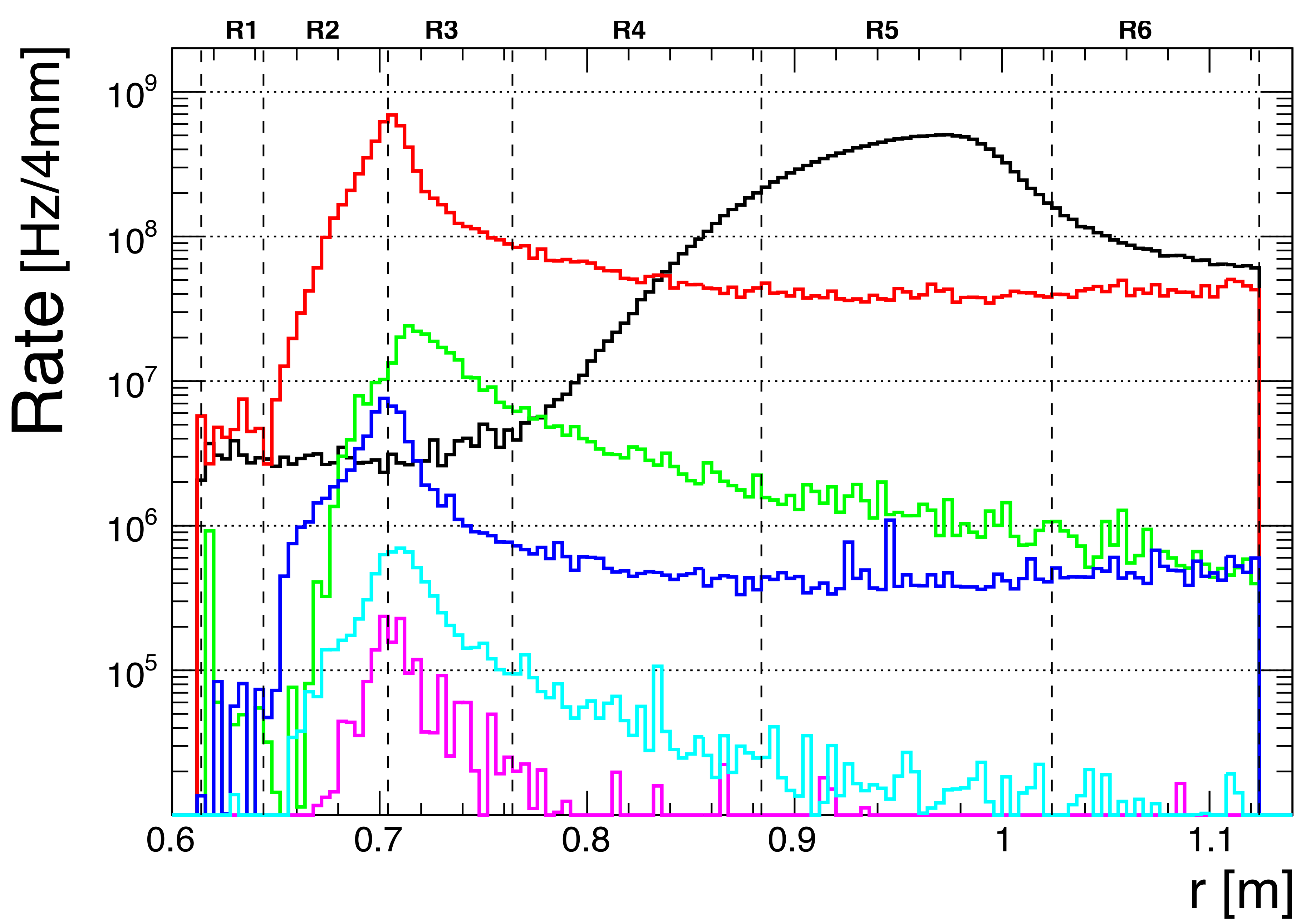

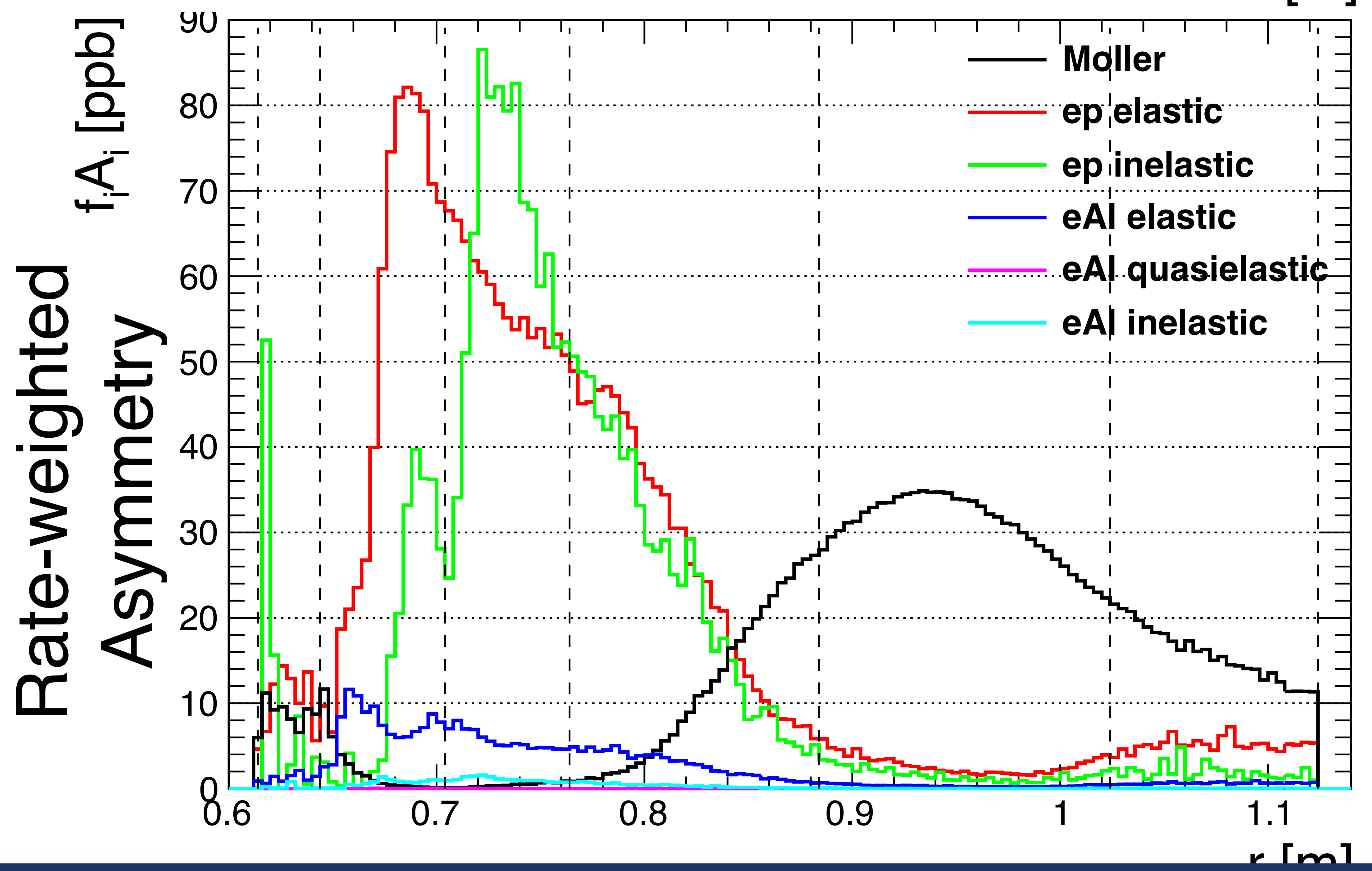

- 16 different tile asymmetries
- “Pre-subtract” Al and pion asymmetry contributions
- Simultaneous fit to 16 measurements with different contributions of e-e, e-p elastic, ep-inelastic
- Extract the “weak charge” for e-e, e-p elastic and inelastic e-p for 3 different W ranges

PV Electron-Proton Inelastic Scattering

electroweak neutral current structure functions

Deep inelastic scattering $A_{PV} = \frac{G_F Q^2}{\sqrt{2}\pi\alpha}\left[a(x) + f(y)b(x)\right]$

$$A_{PV} = \frac{G_F Q^2}{2\sqrt{2}\pi\alpha}\left[g_A \frac{F_1^{\gamma Z}}{F_1^{\gamma}} + g_V \frac{f(y)}{2}\frac{F_3^{\gamma Z}}{F_1^{\gamma}}\right]$$

At high Q^2, one can use quark pdf's and standard model couplings. At forward angles, the prediction is $A_{PV}/Q^2 \sim 8.5 \times 10^{-5}$. However, for very low Q^2, one needs a model as a function of W.

MOLLER kinematics:	**E_{beam} = 11 GeV, $6 < \theta_{lab} < 20$ mrad, E' = 3 to 8 GeV** **Q^2 ~ 0.001 - 0.02 GeV^2, W^2 from 1 to 20 GeV^2**	**Diffractive Regime (VMD or Pomeron Physics)**

Assumption: A_{PV}/Q^2 ~ F(W) is constant in 3 W regions

Mock Fit Extraction with Monte Carlo Trial Data Fit

Processes	Expected A (ppb)	σ_A (ppb)	$\frac{\sigma_A}{\|A\|}$ (%)
Moller	-35.20	0.64	1.8
ep-elastic	-19.67	1.82	9.2
ep-inelastic (1)	-439.94	80.6	18.3
ep-inelastic (2)	-433.96	38.3	8.8
ep-inelastic (3)	-384.59	91.5	23.8
eAl-elastic	297.27	83.01	27.9

- extracted precision close to statistical power for *ee*, factor <2 for backgrounds

Corrections for Ring-5 Tiles after Fit Extraction

Process	Correction (%)	Systematic Error (%)
e-p elastic	1.14	0.08
e-p inelastic ($W < 1.4$ GeV)	-1.34	0.22
e-p inelastic ($1.4 < W < 2.5$ GeV)	-1.54	0.11
e-p inelastic ($W > 2.5$ GeV)	-1.66	0.35
e-Al elastic	0.87	0.09
e-Al other	< 0.10	< 0.10

- precision on backgrounds sufficient for *ee* result

Pion Background

(D. Armstrong)

Pion background (dominantly from real and virtual photoproduction from proton)

Estimate f_π~ 0.13% with A^π_{PV}~ 500 ppb

Need to determine $f_\pi A^\pi_{PV}$ to ~20% relative precision

Range out electrons with Pb absorber - acrylic Cerenkov detectors

- Measure A^π_{PV} with 100 MHz total pion rate over full azimuth in integration mode
- Measure f_π in counting mode, using information from pion detectors as well as tracking, shower-max, and thin quartz MD

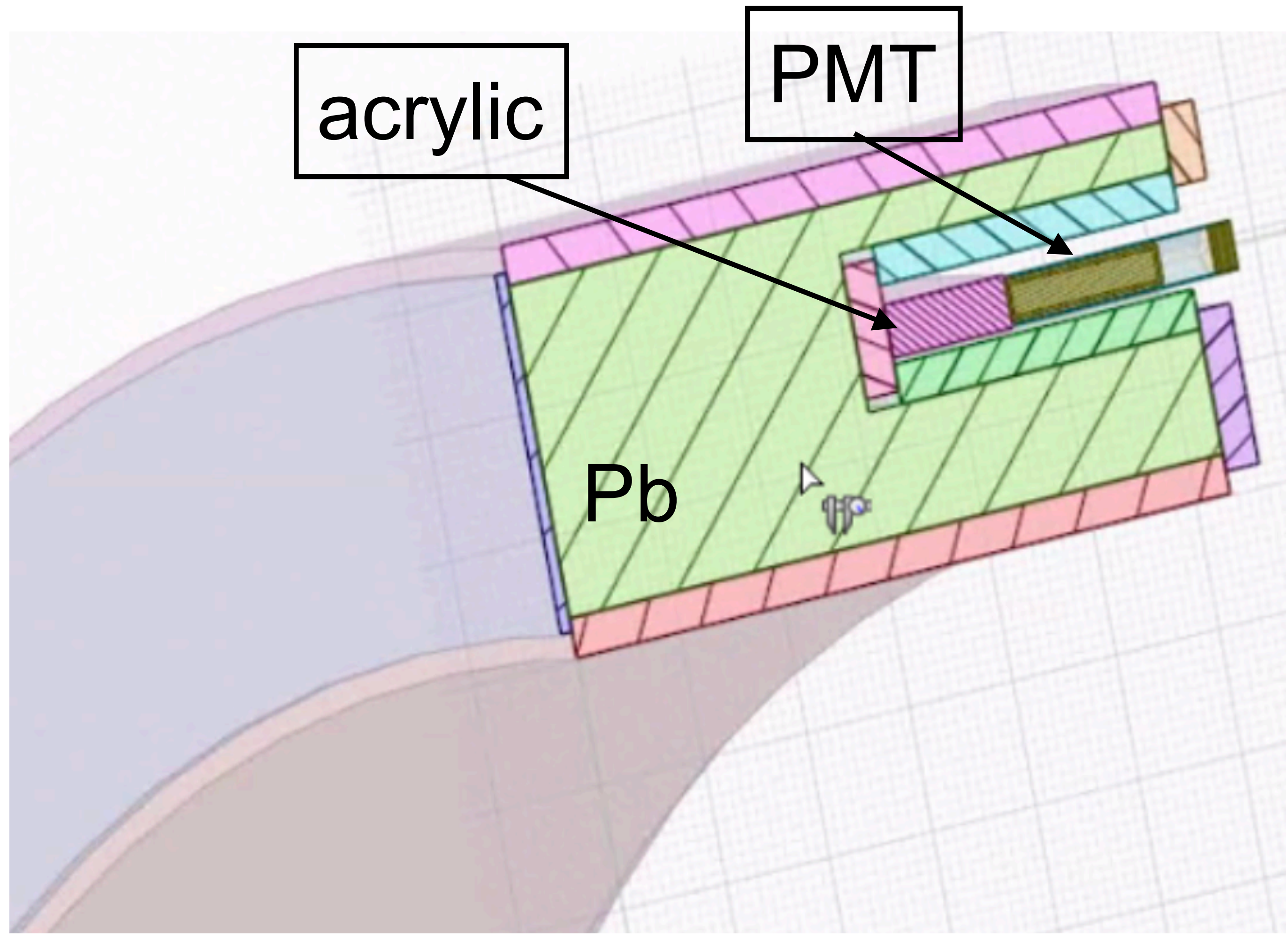

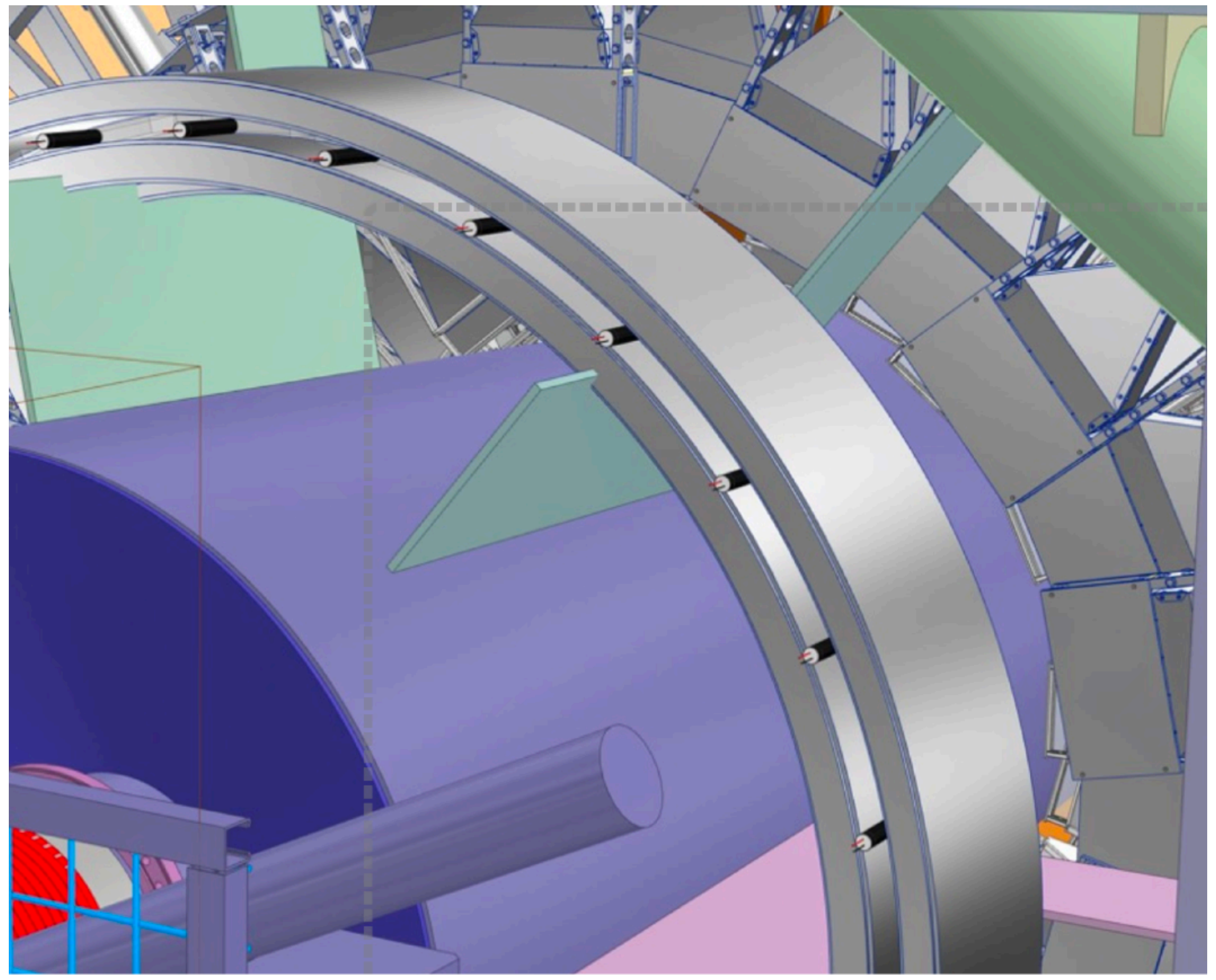

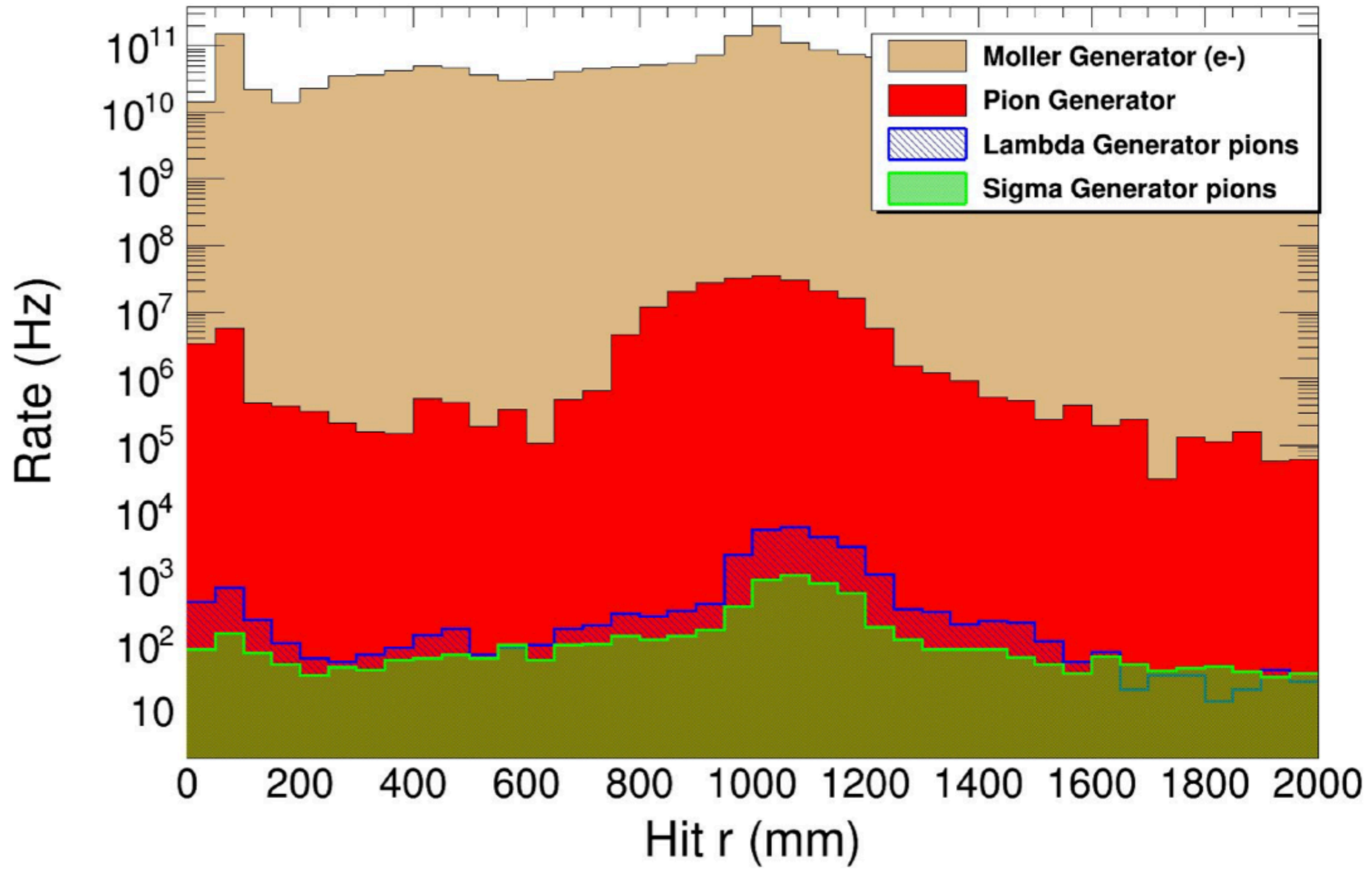

Hyperon generator (with rates based on CLAS data) used to estimate expected pion asymmetries

Polarimetry

- Two independent measurements which can be cross-checked
- Continuous monitoring during production (protects against drifts, precession...)
- Statistical power to facilitate cross-normalization (get to systematics limit in about 1 hour)

Compton (D. Gaskell)

- continuous measurement with high precision
- state-of-the-art: 0.4% (CREX at 2 GeV) doi.org/10.1103/PhysRevC.109.024323
- Independent electron/photon analyses, each expected to reach 0.4%
- Electron Detector to be built (Diamond μstrips and/or HVMAPS)
- DAQ upgrade

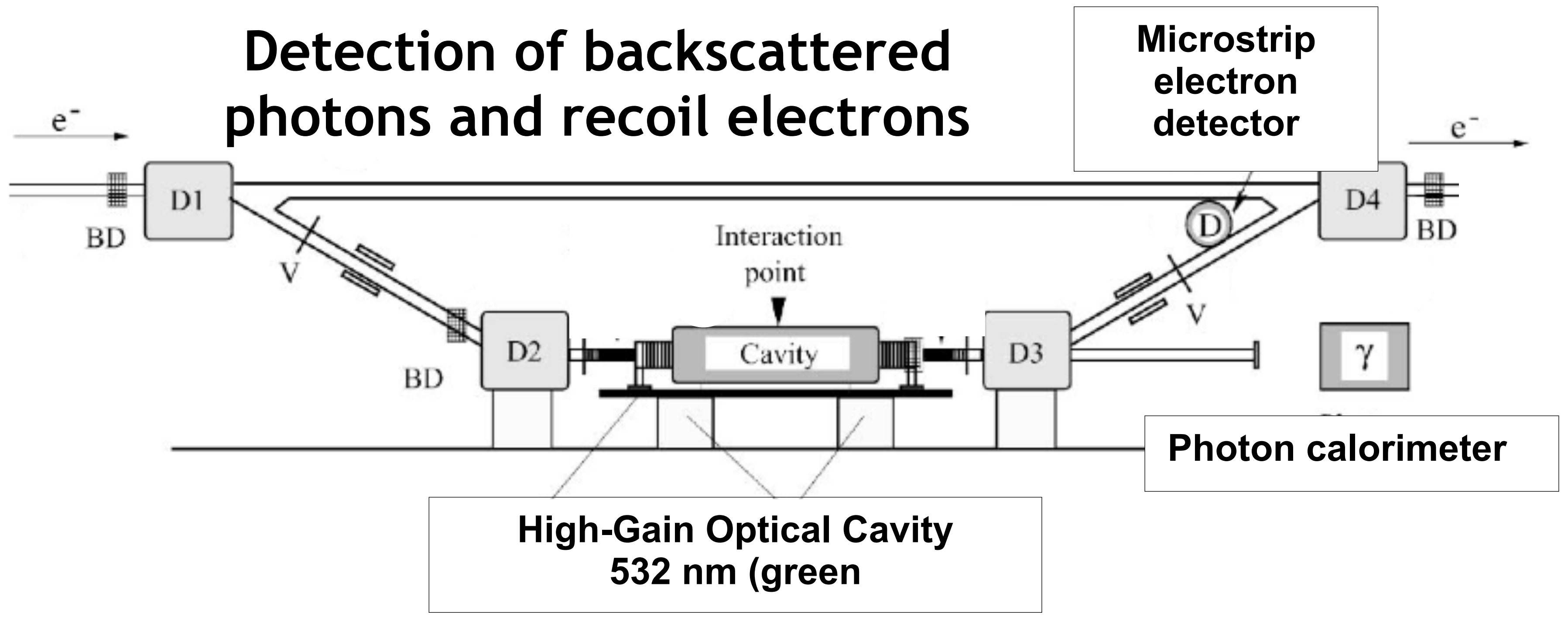

Møller (D. Jones)

- 0.5% instrumental precision for Hall C polarimeter
- Low-current, invasive measurement
- Cross-check with independent uncertainties
- MOLLER project: Collimator, GEM trackers

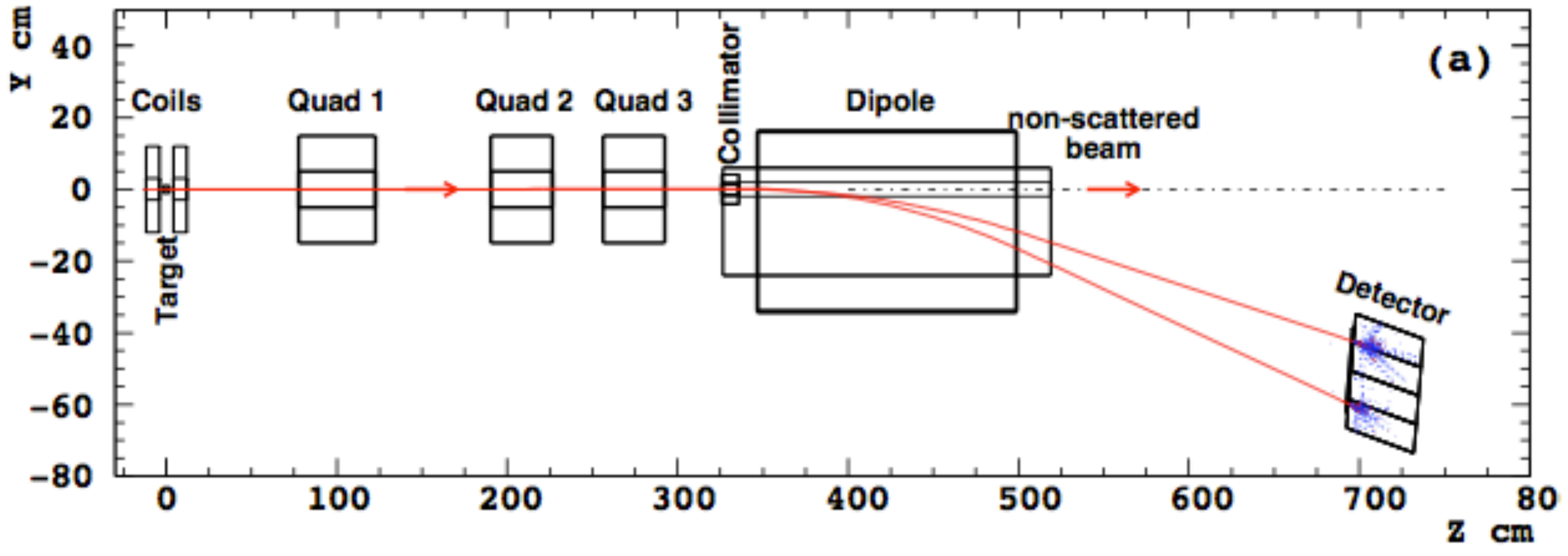

Precision electron beam polarimetry for next generation nuclear physics experiments
K. Aulenbacher, E. Chudakov, **D. Gaskell**, J. Grames, and K. Paschke
Intl J of Mod Phys E Vol. 27, No. 7 (2018) 1830004

Precision Møller polarimetry for PREX-2 and CREX, D.E.King et al.
NIM A 1045 (2023) 167506

Accurate determination of the electron spin polarization in magnetized iron and nickel foils for Møller polarimetry, D.C. Jones et al., NIM A 1043 (2022) 167444

Normalize Kinematics

(D. Armstrong)

$$A_{PV} = mE \frac{G_F}{\sqrt{2}\pi\alpha} \frac{4\sin^2\theta}{(3+\cos^2\theta)^2} Q_W^e$$

Standard model parity-violation analyzing power / weak charge, averaged over acceptance

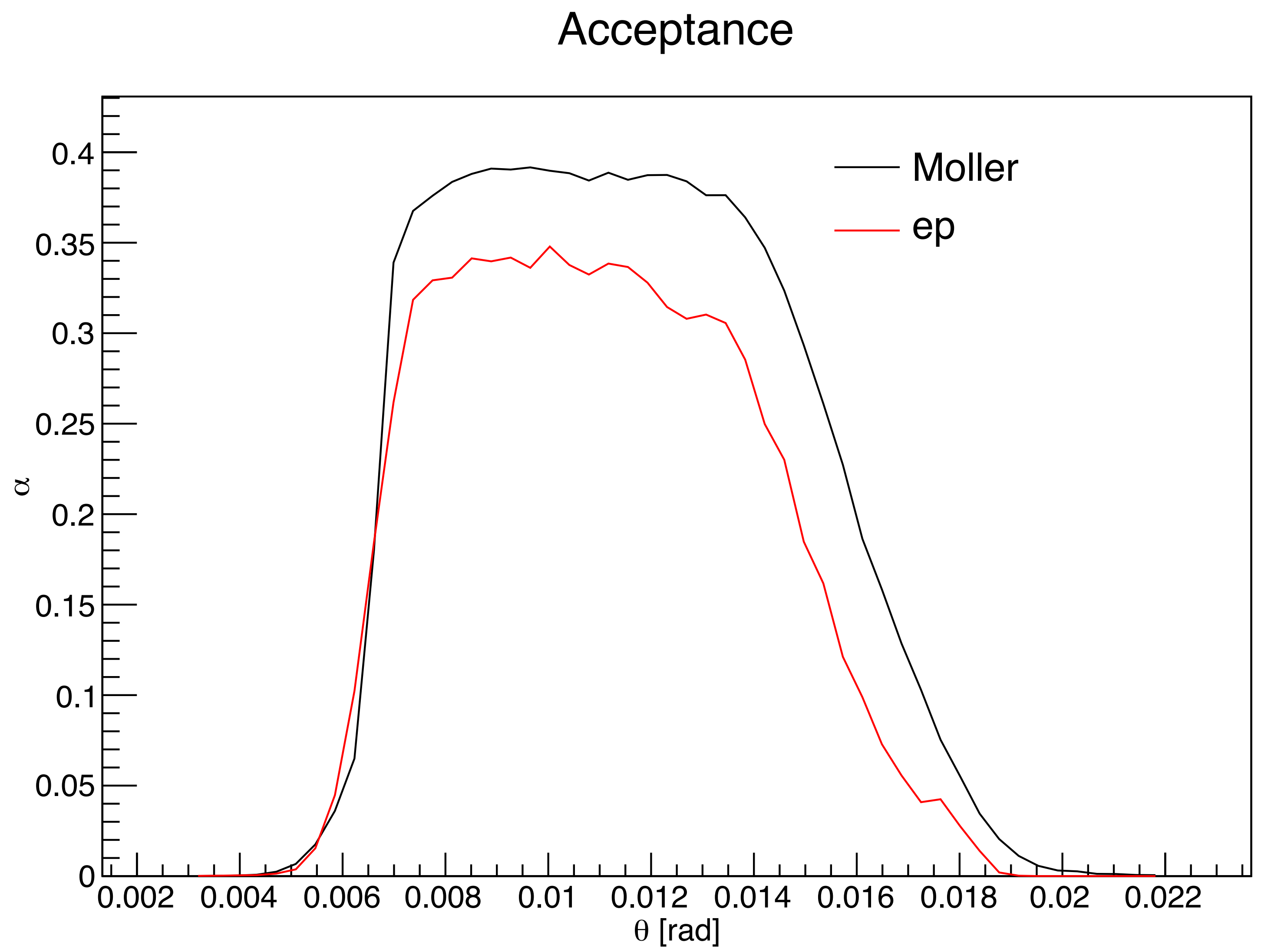

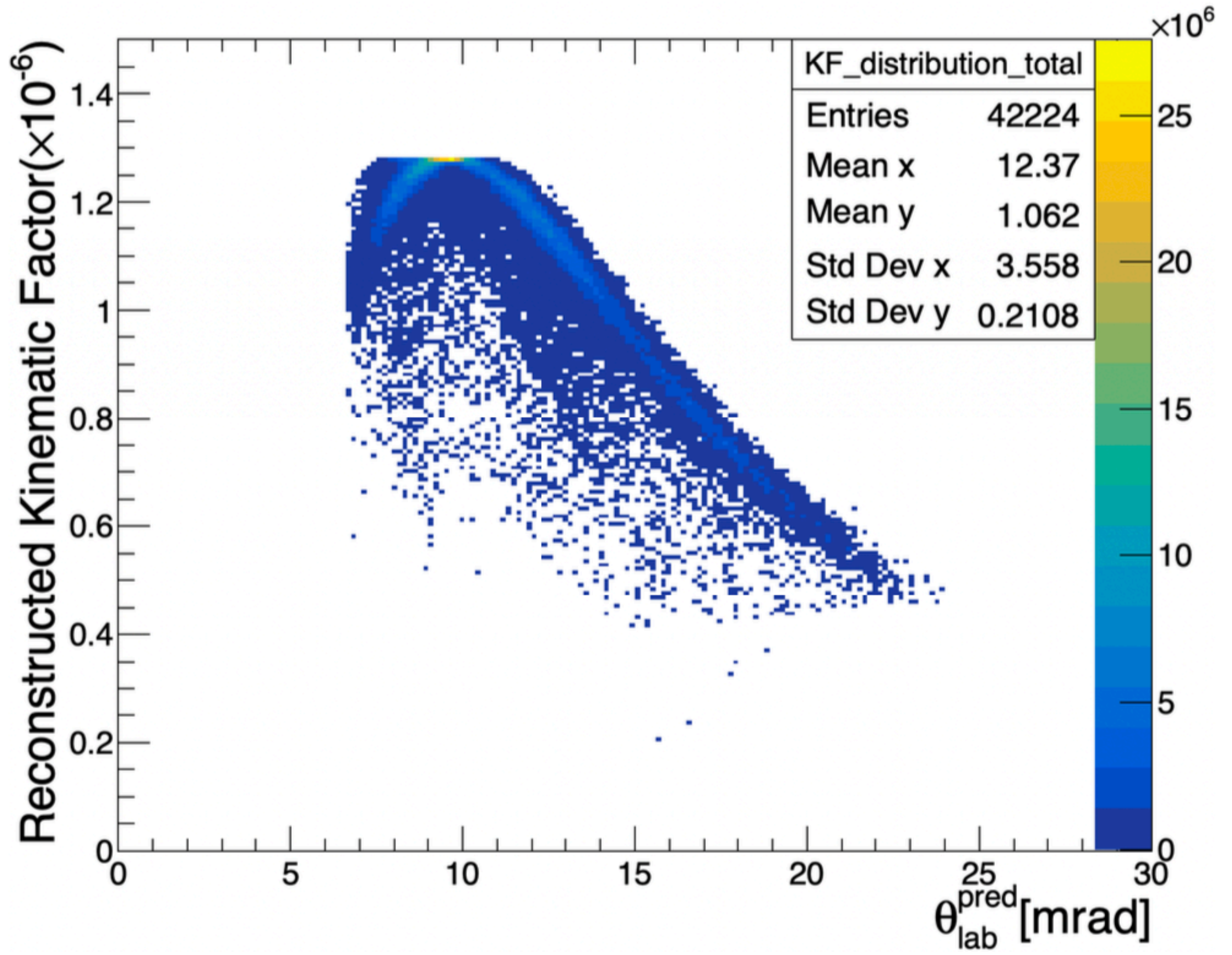

Simulation of acceptance must be benchmarked and checked by tracking measurements

- GEM tracking of event rate from LH2 target
- Demonstrate rate distribution as described by simulation
- Benchmark optics with sieve collimators
- Measure detector position dependent response function (light per hit)

Anticipated Publication

Run Phase 1

- Spectrometer optics, acceptance, alignment
- First look at backgrounds
- Beam monitor resolution
- Beam correction tools
- Beam quality (asymmetry and halo)
- Polarimetry precision

Result: precision of SLAC-E158 on A_{PV}

Run	1 kHz	PAC Days	Stat Error		Efficiency	Calendar Weeks	
Period	Width	(prod)	$\sigma(A_{meas})$	$\sigma(A_{PV})$		(prod)	(calib)
I	101	14	2.96 ppm	11.4%	40%	5	6
II	96	95	1.08 ppm	4.2%	50%	27	3
III	91	235	0.65 ppm	2.5%	60%	56	4
Total		344	0.55	2.1		88	13

Well developed analysis techniques and experienced collaboration.

Plan to publish ee A_T result and A_{PV} result within about one year of finishing Run 1.

Previous experiments released results in about a year, published in about 1.5 years

Result: high precision ee A_T measurement

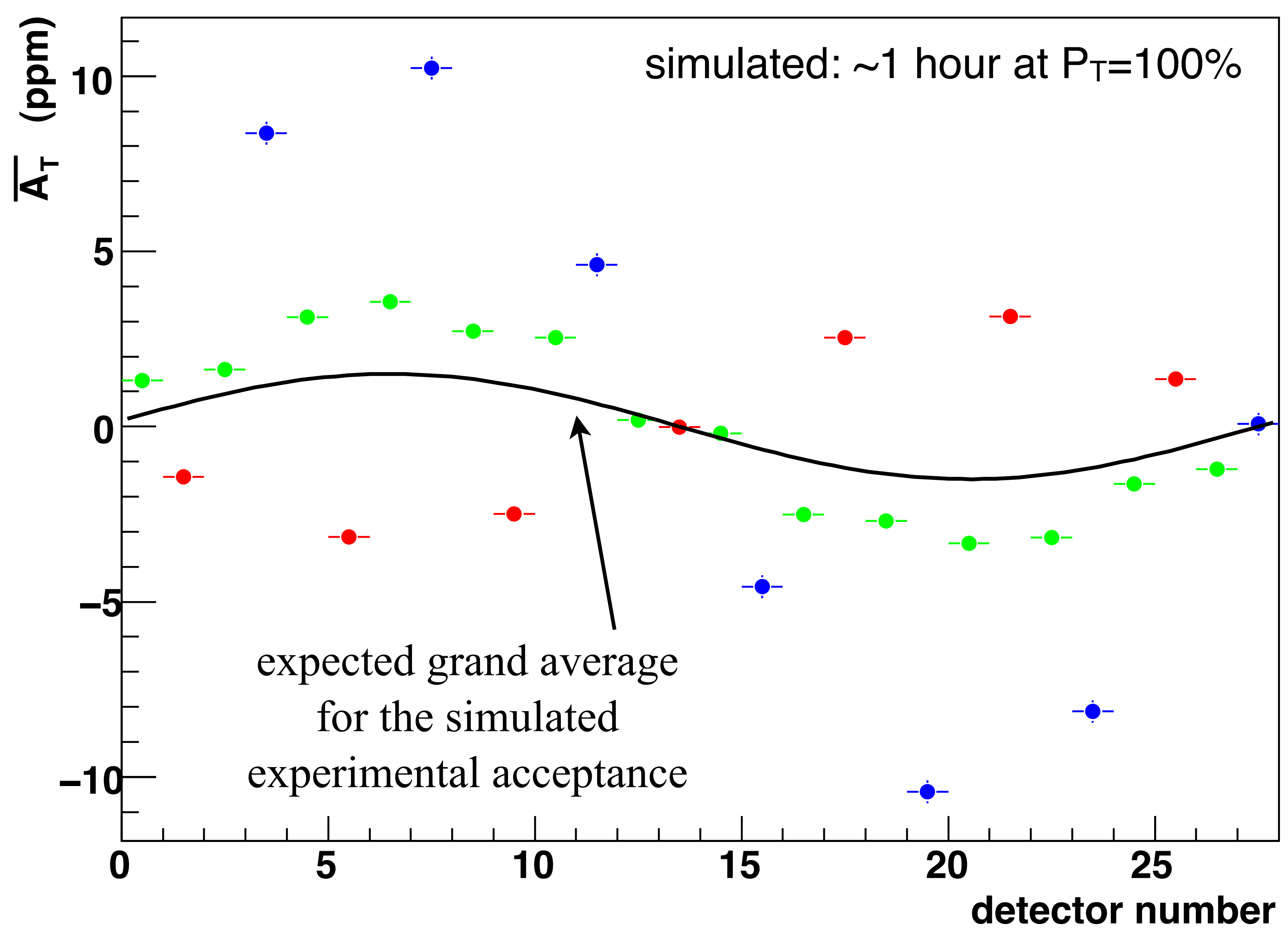

This result should be quick to turn around, ~1 day of data, relatively forgiving systematics

Also: *ep* inelastic A_T

"documented track record"

	running	released	published
E158	Sept 2003	Dec 2004	Apr 2005
PREX-2	ended Aug 2019	Oct 2020	Feb 2021
CREX	ended Sept 2020	Oct 2021	May 2022

Summary

- The collaboration is experienced and has developed and demonstrated effective analysis techniques during recent measurements
- The experimental design has benefited from technologies developed during previous experiments
- Detailed simulation results will assist with analysis development and interpretation
- Run 1 has less demanding systematic goals and a relatively short data collection period. Its analysis will be crucial for guiding future data collection
- The collaboration expects to publish A_T and A_{PV} results within a year of Run 1

Run Period	1 kHz Width	PAC Days (prod)	Stat Error $\sigma(A_{meas})$	Stat Error $\sigma(A_{PV})$	Efficiency	Calendar Weeks (prod)	Calendar Weeks (calib)
I	101	14	2.96 ppm	11.4%	40%	5	6
II	96	95	1.08 ppm	4.2%	50%	27	3
III	91	235	0.65 ppm	2.5%	60%	56	4
Total		344	0.55	2.1		88	13

Error Source	Fractional Error (%) Run 1	Fractional Error (%) Ultimate
Statistical	**11.4**	**2.1**
Absolute Norm. of the Kinematic Factor	3	0.5
Beam (second moment)	2	0.4
Beam polarization	1	0.4
$e + p(+\gamma) \rightarrow e + X(+\gamma)$	2	0.4
Beam (position, angle, energy)	2	0.4
Beam (intensity)	1	0.3
$e + p(+\gamma) \rightarrow e + p(+\gamma)$	0.6	0.3
$\gamma^{(*)} + p \rightarrow (\pi, \mu, K) + X$	1.5	0.3
$e + Al(+\gamma) \rightarrow e + Al(+\gamma)$	0.3	0.15
Transverse polarization	2	0.2
Neutral background (soft photons, neutrons)	0.5	0.1
Linearity	0.1	0.1
Total systematic	**5.5**	**1.1**

Appendix

Phased Approach to Achieving Ultimate Precision

Run Period	1 kHz Width	PAC Days (prod)	Stat Error $\sigma(A_{meas})$	Stat Error $\sigma(A_{PV})$	Efficiency	Calendar Weeks (prod)	Calendar Weeks (calib)
I	101	14	2.96 ppm	11.4%	40%	5	6
II	96	95	1.08 ppm	4.2%	50%	27	3
III	91	235	0.65 ppm	2.5%	60%	56	4
Total		344	0.55	2.1		88	13

Progressively improve statistical power

Run Period	I	II	III
1 kHz Width Goal	101 ppm	96 ppm	91ppm
Width over counting statistics	23%	17%	11%
Excess noise over counting statistics	59 ppm	50 ppm	40 ppm
Allowance over ultimate goal	44 ppm	31 ppm	–

and systematic control

Error Source	Fractional Error (%) Run 1	Fractional Error (%) Ultimate
Statistical	**11.4**	**2.1**
Absolute Norm. of the Kinematic Factor	3	0.5
Beam (second moment)	2	0.4
Beam polarization	1	0.4
$e + p(+\gamma) \to e + X(+\gamma)$	2	0.4
Beam (position, angle, energy)	2	0.4
Beam (intensity)	1	0.3
$e + p(+\gamma) \to e + p(+\gamma)$	0.6	0.3
$\gamma^{(*)} + p \to (\pi, \mu, K) + X$	1.5	0.3
$e + Al(+\gamma) \to e + Al(+\gamma)$	0.3	0.15
Transverse polarization	2	0.2
Neutral background (soft photons, neutrons)	0.5	0.1
Linearity	0.1	0.1
Total systematic	**5.5**	**1.1**

Run Phase 1

- Spectrometer optics, acceptance, alignment
- First look at backgrounds
- Beam monitor resolution
- Beam correction tools
- Beam quality (asymmetry and halo)
- Polarimetry precision

Result: precision of SLAC-E158

Run Phase 2

- statistical behavior of measured asymmetries
- quality of “slow” reversals (Wien, g-2)
- precision on background, normalization, beam corrections, polarization

Result: 2.5x beyond SLAC-E158, $\delta(\sin^2\theta_W)$=0.00044 (stat), 0.00047 (stat+syst)

Run Phase 3

- ultimate precision, ultimate systematic uncertainty

Result: $\delta(\sin^2\theta_W)$=0.00024 (stat), 0.00028 (stat+syst)

The Box Diagram Connection

Radiative corrections to the theoretical prediction of the weak charge of the proton

$$Q_W^p = (1 + \Delta\rho + \Delta_e)\left(1 - 4\sin^2\theta_W(0) + \Delta_e'\right) + \Box_{WW} + \Box_{ZZ} + \Box_{\gamma Z}(0)$$

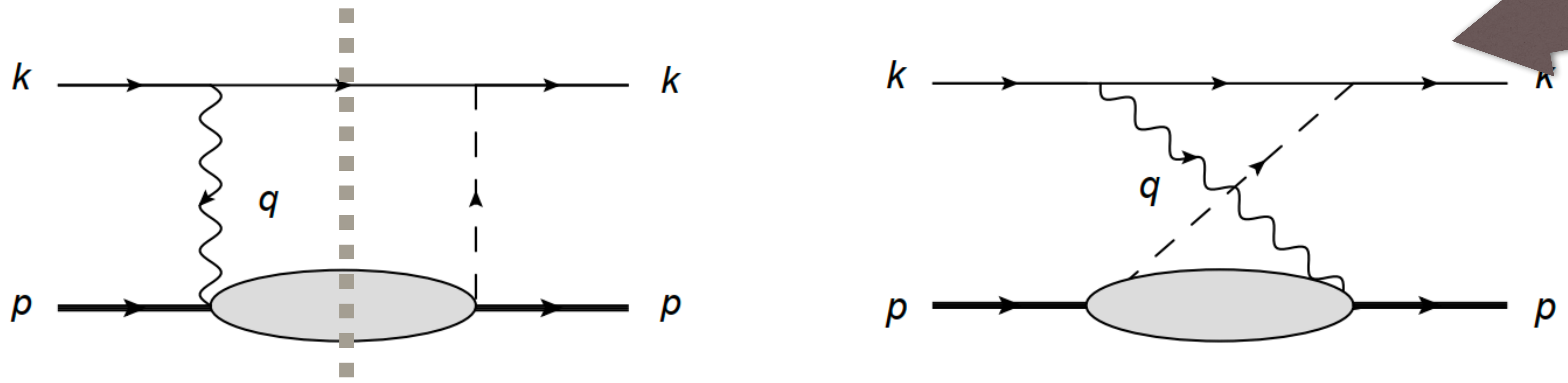

$F_{1,2}^{\gamma Z}(Q^2, W^2)$

In 3 different kinematic regimes

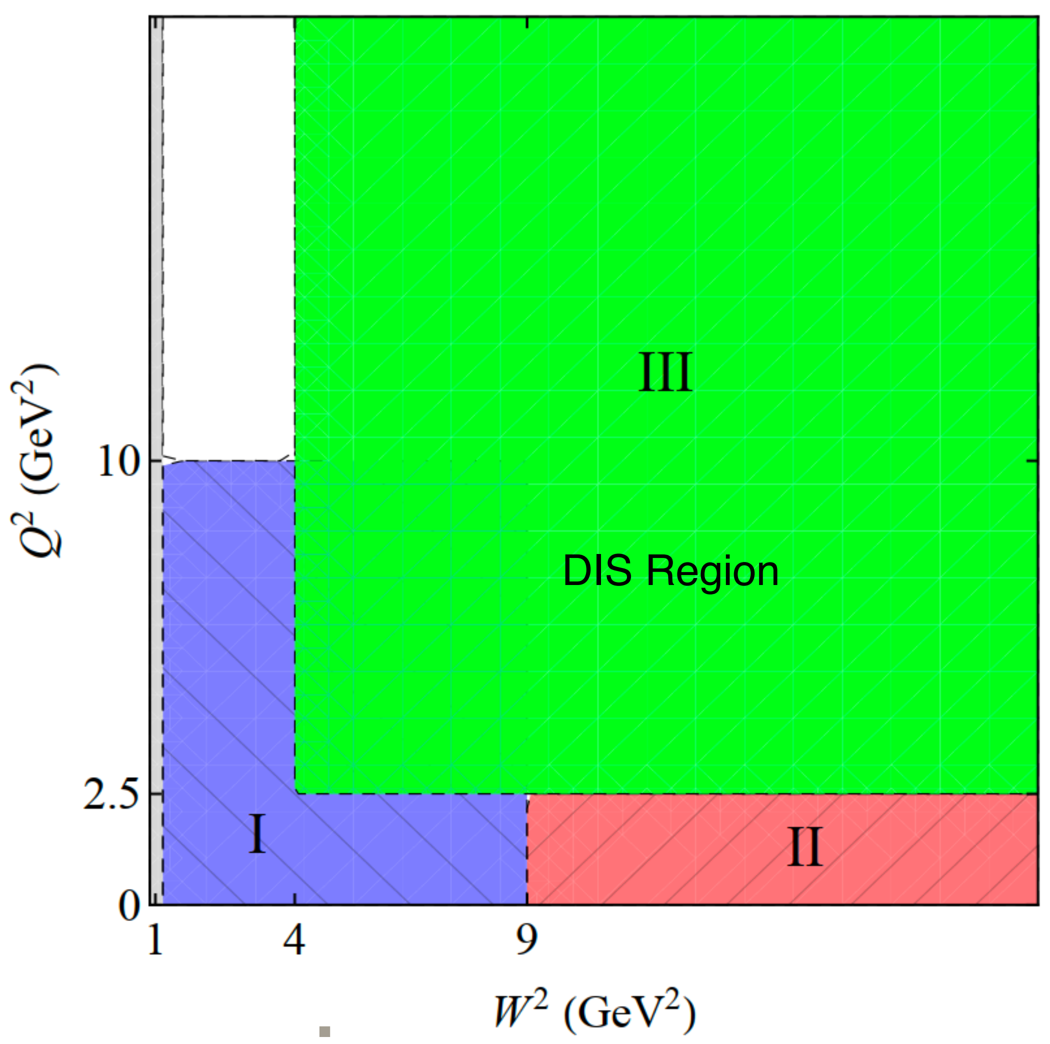

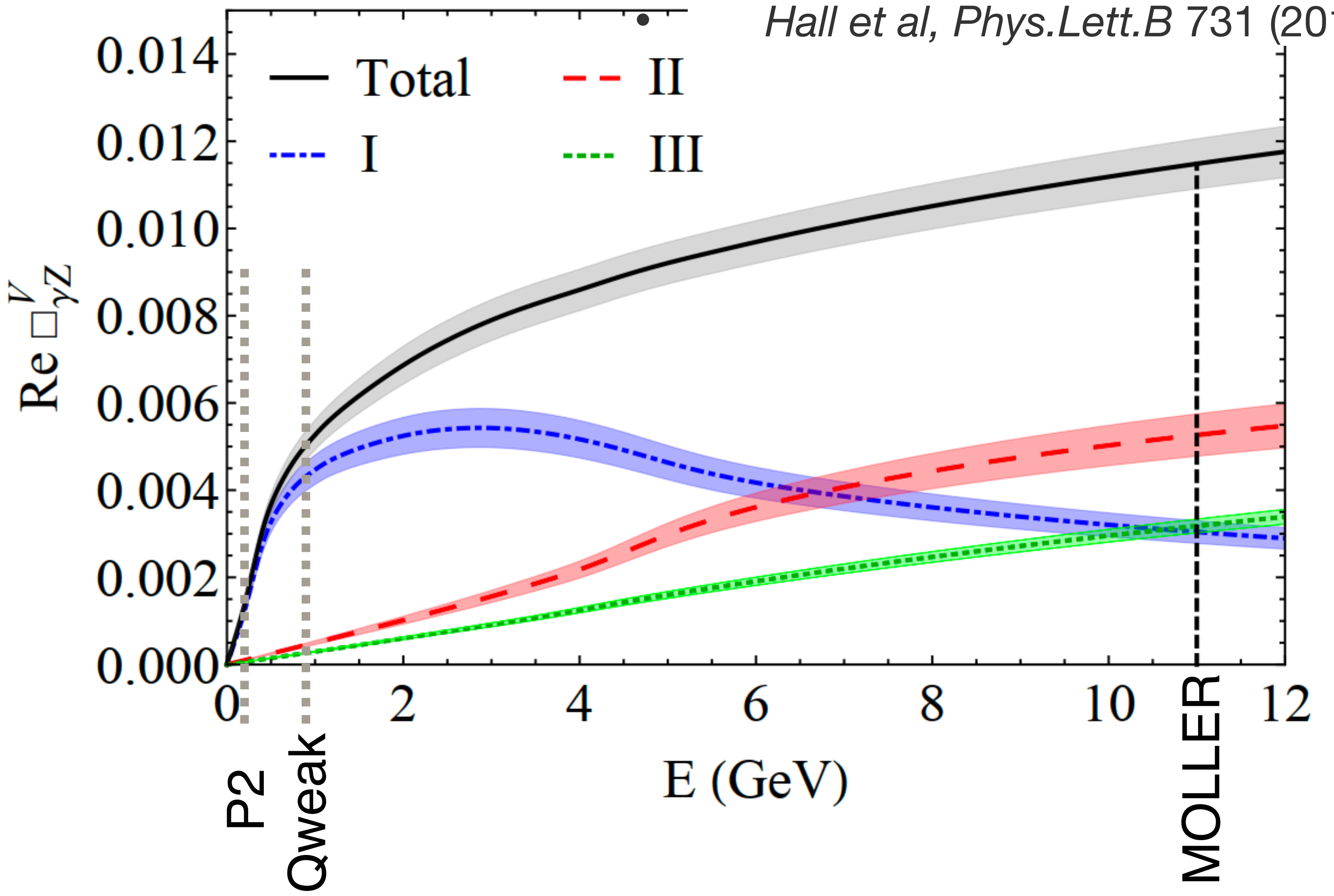

Hall et al, Phys.Lett.B 731 (2014) 287-292, *Phys.Lett.B* 733 (2014)

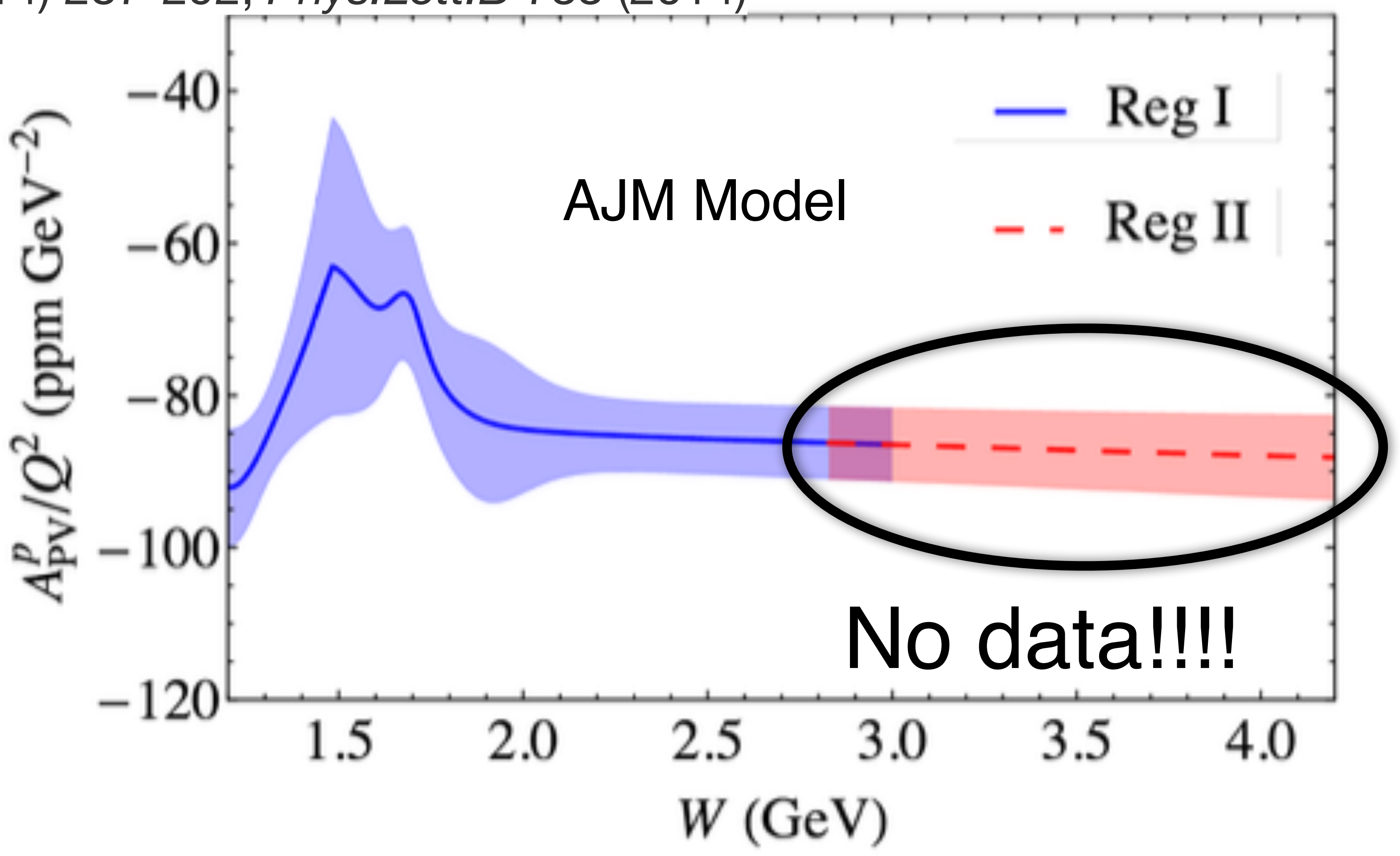

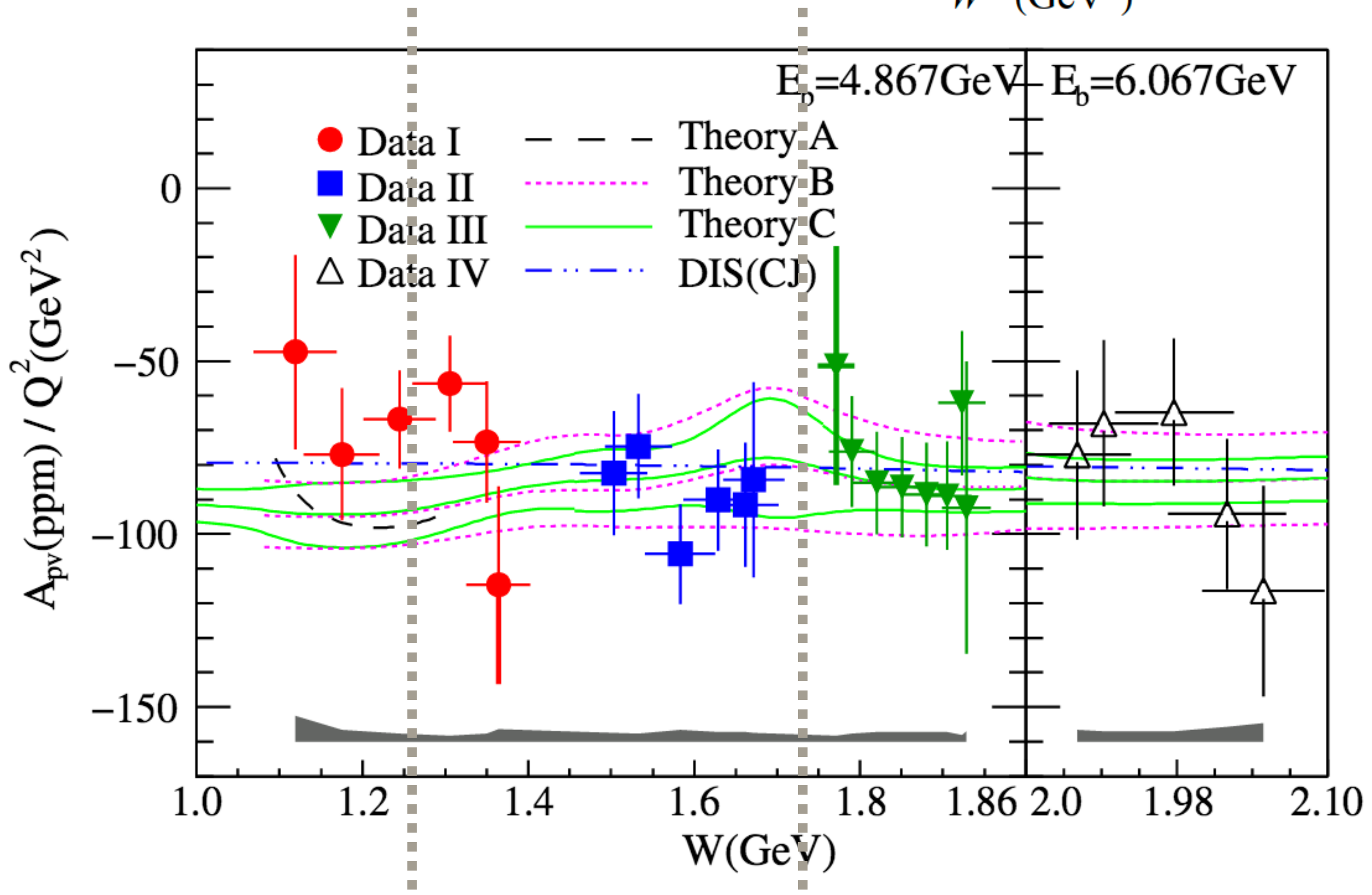

Matsui et al, Gorschein et al, AJM, CJ, compared to PVDIS measurements

There is no data on $F_1^{\gamma Z}$ in Region II! MOLLER will make the first ever measurement!

Table 1: *Nominal parameters for the conceptual design of the MOLLER experimental apparatus.*

Parameter	Value
E [GeV]	≈ 11.0
E' [GeV]	2.0 - 9.0
$\theta_{\rm CM}$	50°-130°
$\theta_{\rm lab}$	0.26°-1.2°
$\langle Q^2 \rangle$ [GeV^2]	0.0058
Maximum Current [μA]	70
Target Length (cm)	125
ρ_{tgt} [g/cm^3] (T= 20K, P = 35 psia)	0.0715
Max. Luminosity [cm^{-2} sec^{-1}]	$2.4 \cdot 10^{39}$
σ [μbarn]	≈ 60
Møller Rate @ 65 μA [GHz]	≈ 134
Statistical Width(1.92 kHz flip) [ppm/pair]	≈ 91
Target Raster Size [mm $\times$ mm]	5×5
Production running time	344 PAC-days = 8256 hours
ΔA_{raw} [ppb]	≈ 0.54
Background Fraction	≈ 0.10
$P_{\rm B}$	$\approx 90\%$
$\langle A_{PV} \rangle$ [ppb]	≈ 32
$\Delta A_{stat} / \langle A_{expt} \rangle$	2.1%
$\delta(\sin^2 \theta_W)_{stat}$	0.00023

Emittance Growth and Spot Size

Spot-size helicity dependence in hall diluted by synchrotron emittance growth contribution

helicity dependent spot size in injector $\sigma_{(inj)R,L}$

Spot-size "noise" from synchrotron σ_{synch}

incoherent growth, so width is quadrature sum $\sigma^2_{R,L} = \sigma^2_{synch} + \sigma^2_{(inj)R,L}$

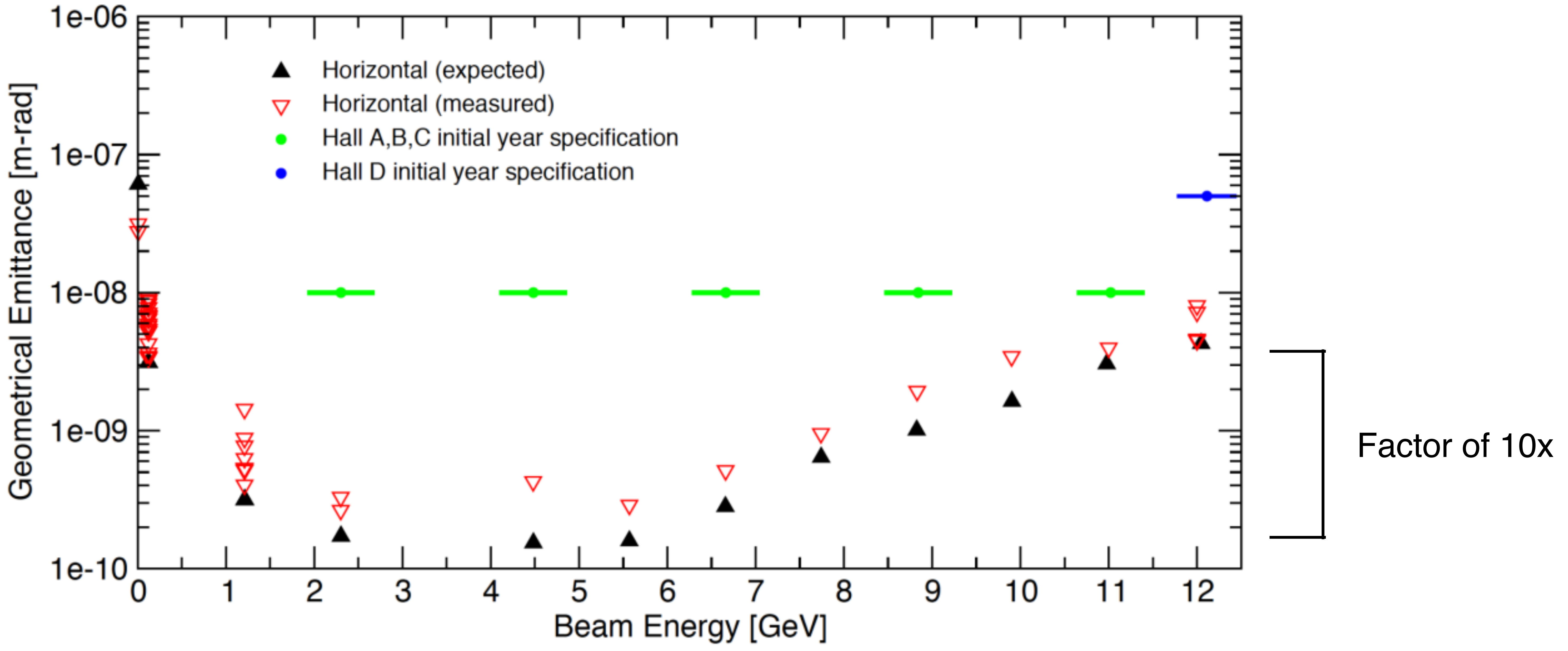

Background Hygiene: design for “2-bounce”

Avoid “1-bounce” line-of-sight to target

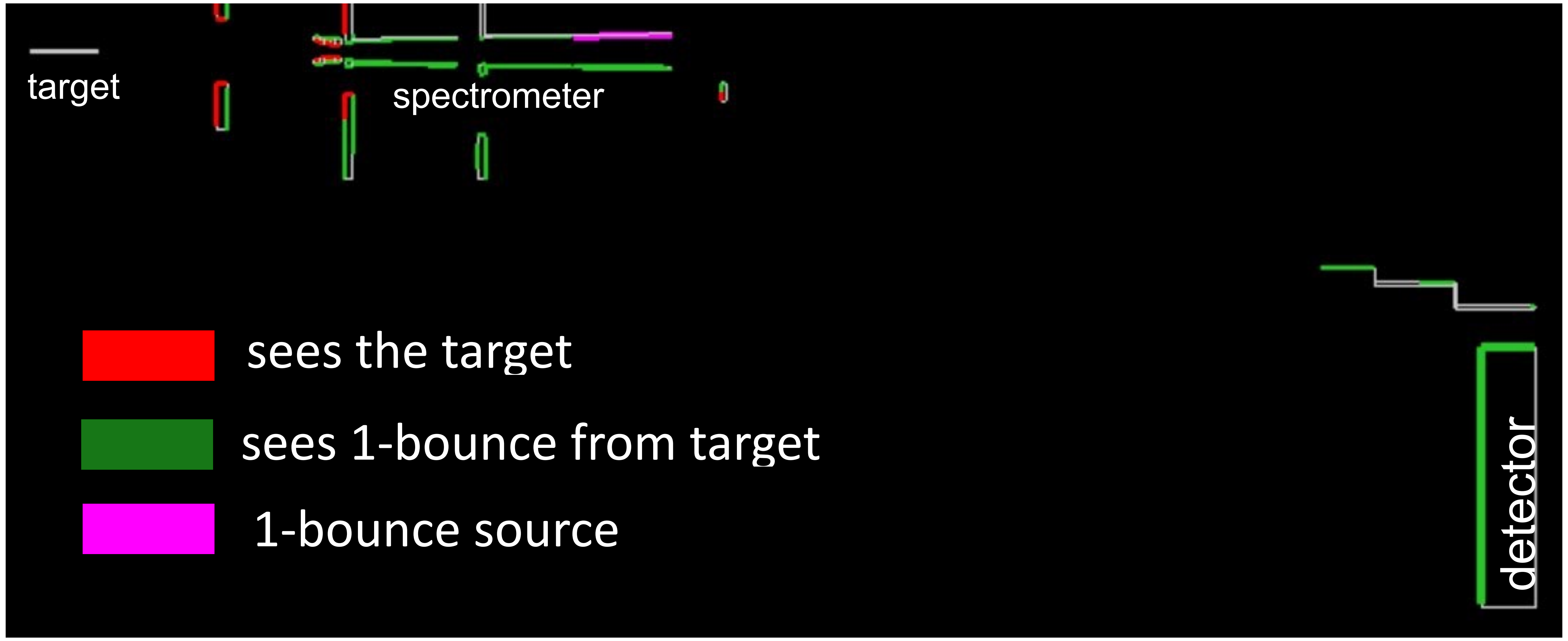

- Python code
  - Target, collar, collimators, beam shields, detector (600, 690-1300 mm)
  - Uses straight lines to simulate an isotropic source (with random position, angle)
  - Surfaces that “see” the target (red) become new sources
  - Make it so detectors see no red surfaces
- Tolerance study
  - move the collimators and/or coils by +/-1 mm w/o seeing green on the detectors

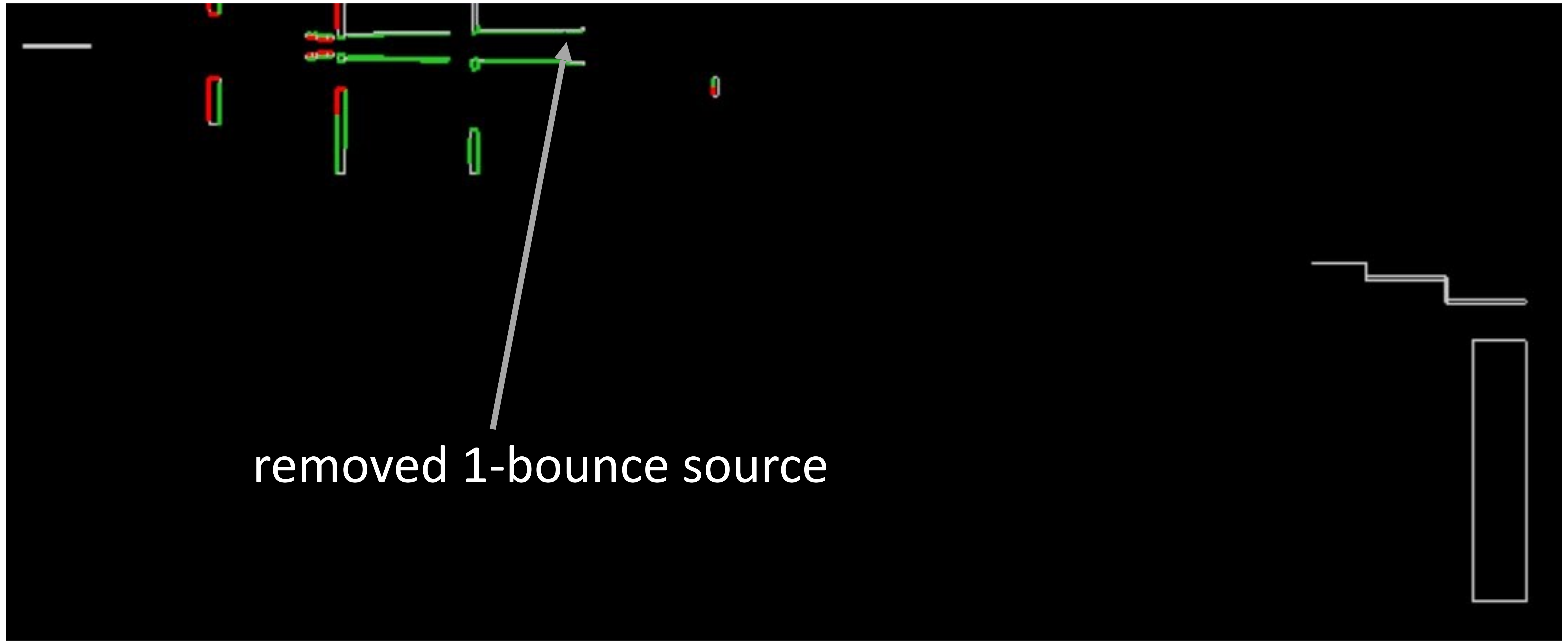

Remoll Generator

- Generates e', K+, and Y (Λ or Σ)
  - Fixed 11 GeV e beam (needs updated to a realistic beam profile).
  - Thrown flat in $\theta_{e'}$, $\phi_{e'}$, $E_{e'}$, $\theta^{CM}_{K'}$ and $\phi^{CM}_{K'}$.
- Rates calculated using the CLAS data done at the analysis step after remoll simulation.
  - Allows for changes to be made to the rates without needing to generate new MC samples.

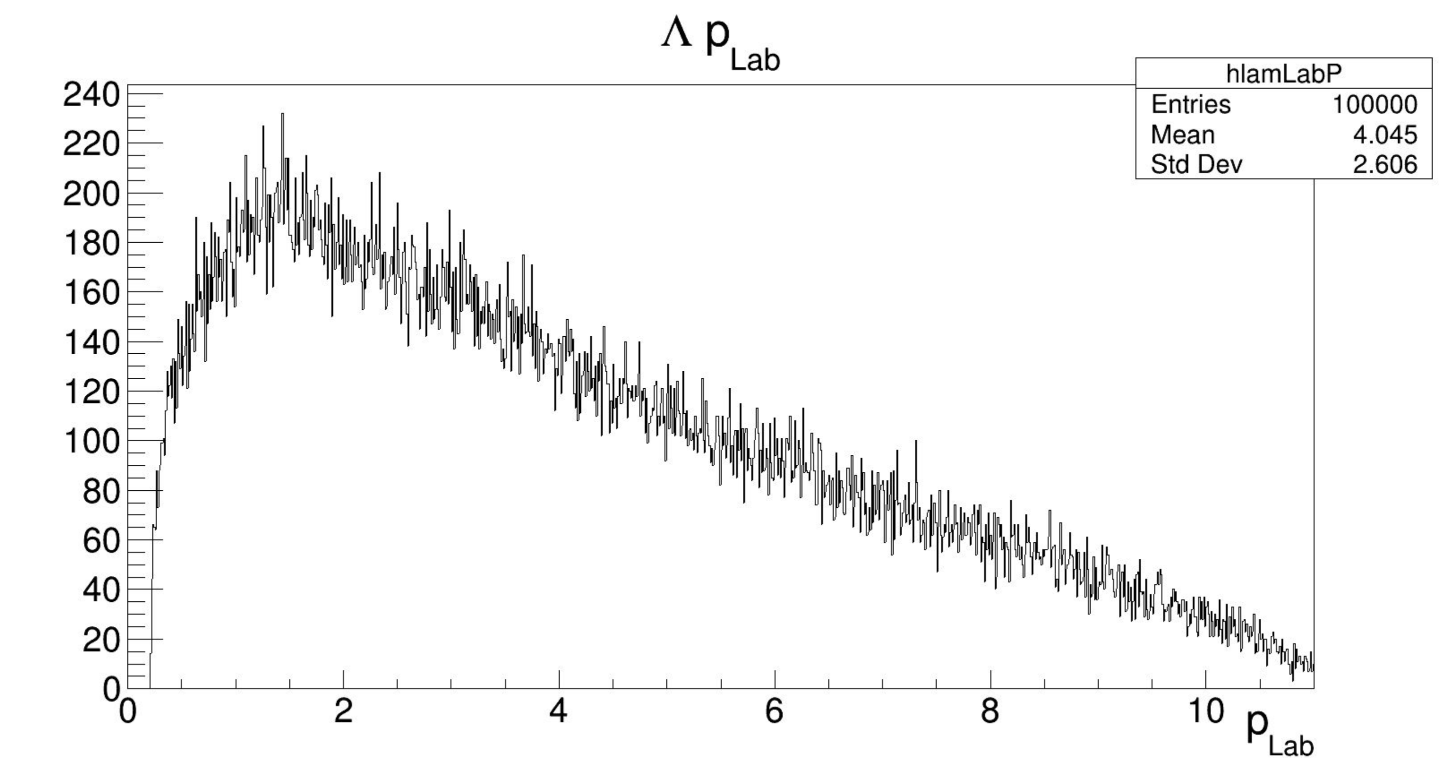

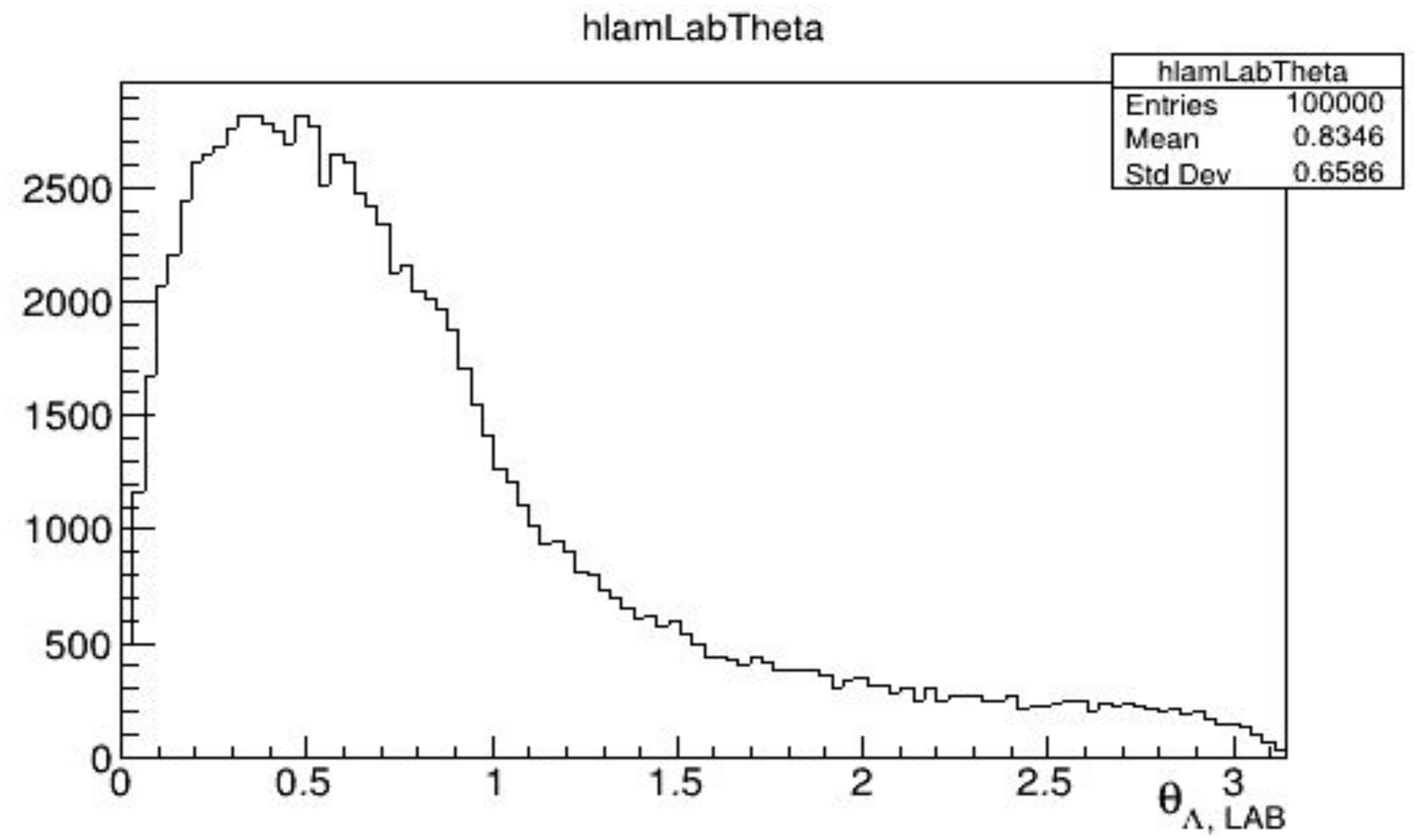

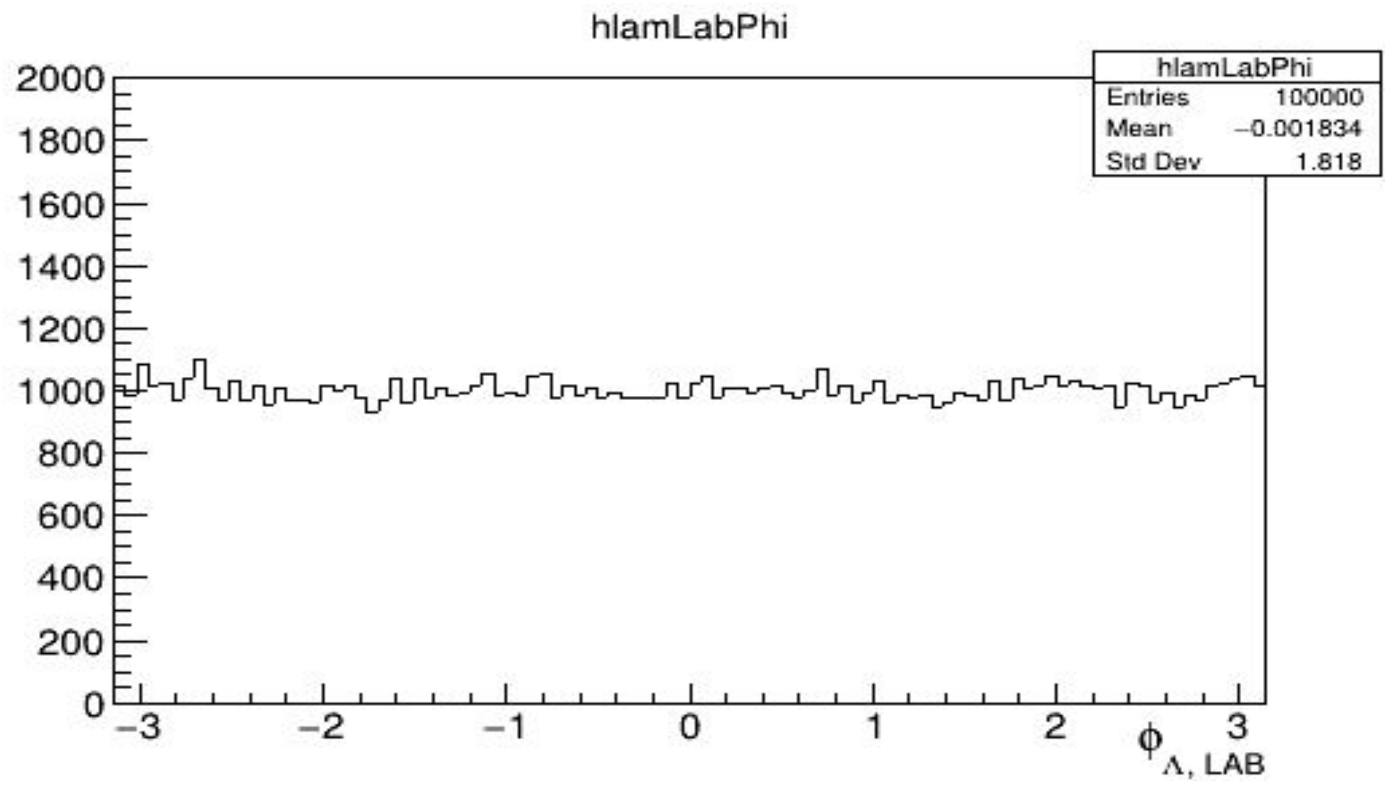

Published CLAS Data (Q^2=1.8 GeV^2) example

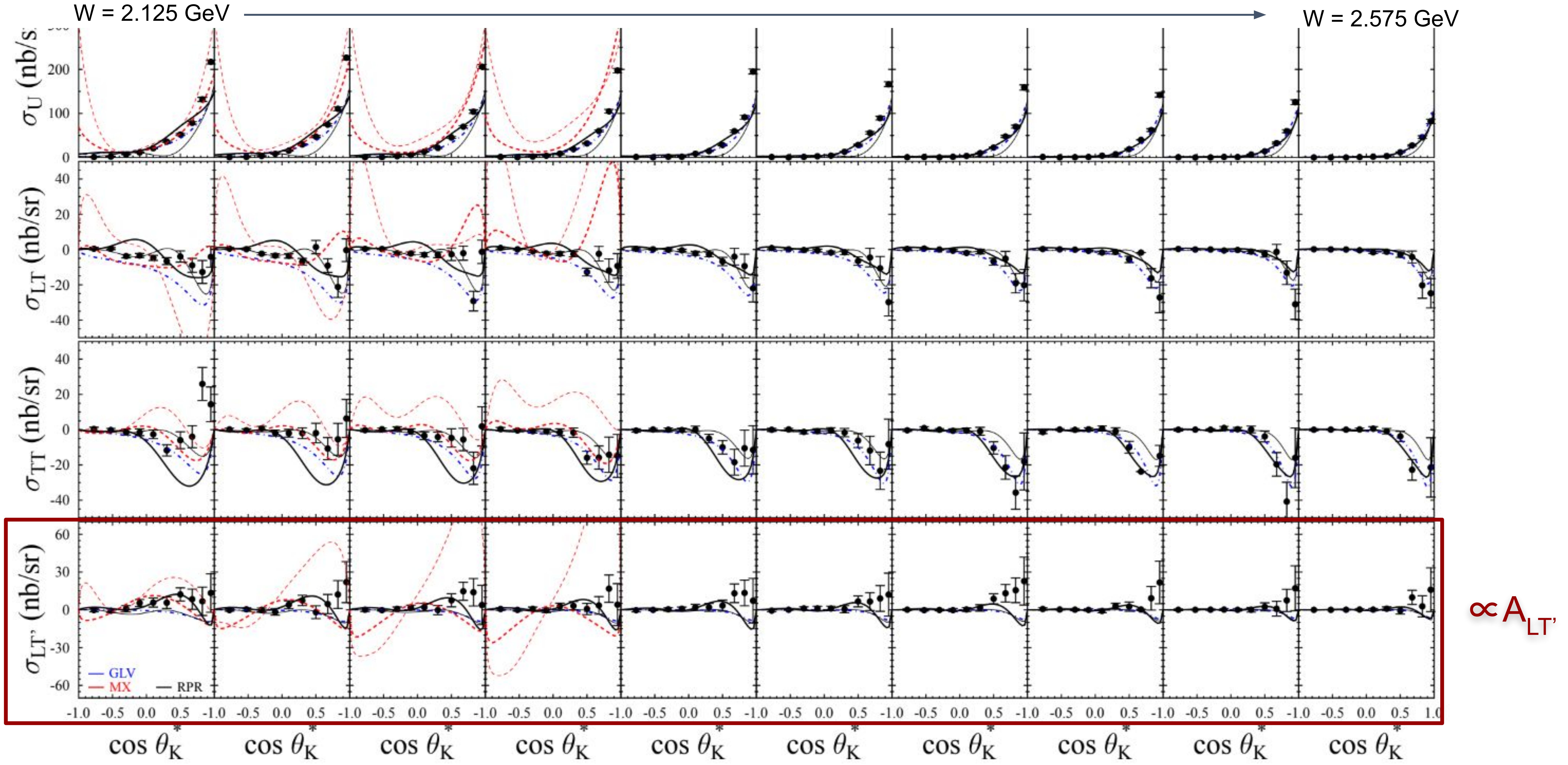

FIG. 13: (Color online) Structure functions σ_U, σ_{LT}, σ_{TT}, and $\sigma_{LT'}$ (in nb/sr) for $K^+\Lambda$ production vs. $\cos\theta_K^*$ at 5.499 GeV for Q^2=1.80 GeV^2 and W from 2.125 to 2.575 GeV. The error bars represent the statistical uncertainties only. The curves are defined in the caption of Fig. 12.

https://doi.org/10.48550/arXiv.1212.1336